RSC Advances

REVIEW

View Article Online
View Journal | View Issue

Cite this: *RSC Adv.*, 2026, **16**, 15119

Advancement in photocatalytic degradation of ciprofloxacin: mechanisms, materials and environmental remediation

Laraib Asad,[a] Zia Ul Haq Khan *[a] and Fida Ullah[b]

Received 3rd January 2026
Accepted 8th March 2026

DOI: 10.1039/d6ra00060f

rsc.li/rsc-advances

Ciprofloxacin (CIP), a widely used fluoroquinolone antibiotic, poses significant ecological risks due to its persistence in water systems and contribution to antibiotic resistance. Traditional wastewater treatment methods are ineffective in completely degrading CIP, necessitating more advanced solutions. This review explores the potential of photocatalytic degradation as a promising approach for CIP removal, focusing on the generation of reactive oxygen species (ROS) using various photocatalysts. The influence of operational parameters such as catalyst type, CIP dosage, pH, temperature, and light source on degradation efficiency is critically evaluated. Recent advancements in visible-light-responsive photocatalysts and hybrid treatment systems are discussed, along with their performance metrics. The paper concludes with future directions for developing novel materials and integrated systems to enhance environmental remediation, offering a comprehensive evaluation of the photocatalytic degradation process of CIPs.

1. Introduction

1.1. Background and environmental concerns

Ciprofloxacin (Fig. 1) is a popular second-generation fluoroquinolone antibiotic.[1] Considering the carboxylic acid group and the basic-N-moiety, the acid disintegration constant pK_a readings of CIP species are 5.9 ± 0.15 and 8.89 ± 0.11, respectively. Because of the charge equilibrium of the two aforementioned groups (Fig. 2), the zwitterionic form is the dominant type between pH values of 5.9 and 8.89.[2,3] The piperazine moiety and fluorinated quinolone backbone that make up CIP's structural makeup give it potent antibacterial activity, high chemical stability, and the ability to resist biodegradation. Because of its clinical effectiveness and comparatively low toxicity, fluoroquinolone use has grown dramatically over the last 20 years on a global scale.[4,5] While CIP is highly effective in treating bacterial infections in humans and animals, a large portion of the administered dose is excreted unmetabolized in urine and feces, making its way into wastewater systems.[6–8] Unfortunately, conventional wastewater treatment methods are ineffective in completely removing CIP, resulting in its accumulation in rivers, lakes, and groundwater. The environmental persistence of CIP is attributed to its high chemical stability, low biodegradability, and photostability, which make it resistant to natural degradation processes.[9,10] Furthermore, CIP is considered a pseudo-persistent pollutant, meaning that despite its moderate individual half-life, it continuously enters ecosystems due to prolonged human and veterinary use.[11,12] The presence of CIP in water bodies is particularly concerning because it can disrupt aquatic microbial communities, affect nutrient cycling, and contribute to the development of antibiotic-resistant bacteria. These factors make CIP a priority compound for environmental remediation.[13,14] Given these environmental and public health risks, this study focuses on ciprofloxacin as a model contaminant for exploring advanced degradation methods, specifically photocatalytic degradation, as a potential solution to mitigate its environmental impact.[15–19] Some key advantages of photocatalysis over other treatments are summarized in Fig. 3.

1.2. Limitations of existing wastewater treatment approaches

Traditional wastewater treatment plants, which are primarily engineered to eliminate suspended solids, organic load, and pathogens, are not specifically equipped to remove pharmaceutical pollutants such as ciprofloxacin (CIP).[20,21] Physical separation techniques such as sedimentation, filtration, and adsorption onto activated carbon can temporarily reduce CIP concentrations; however, they merely transfer the pollutant to another phase, resulting in concentrated secondary waste that still requires proper disposal.[22,23] Activated sludge systems and other biological treatment techniques are generally ineffective against fluoroquinolones due to their low biodegradability and high resistance to microbial enzymatic attack.[24] Chemical

[a]*Department of Chemistry, COMSATS University Islamabad, Islamabad Campus, Park Road, 45550, Pakistan. E-mail: ziaulhaqkhan11@gmail.com*
[b]*State Key Laboratory of Chemical Resource Engineering, College of Chemistry, Beijing University of Chemical Technology, Beijing, 100029, China*

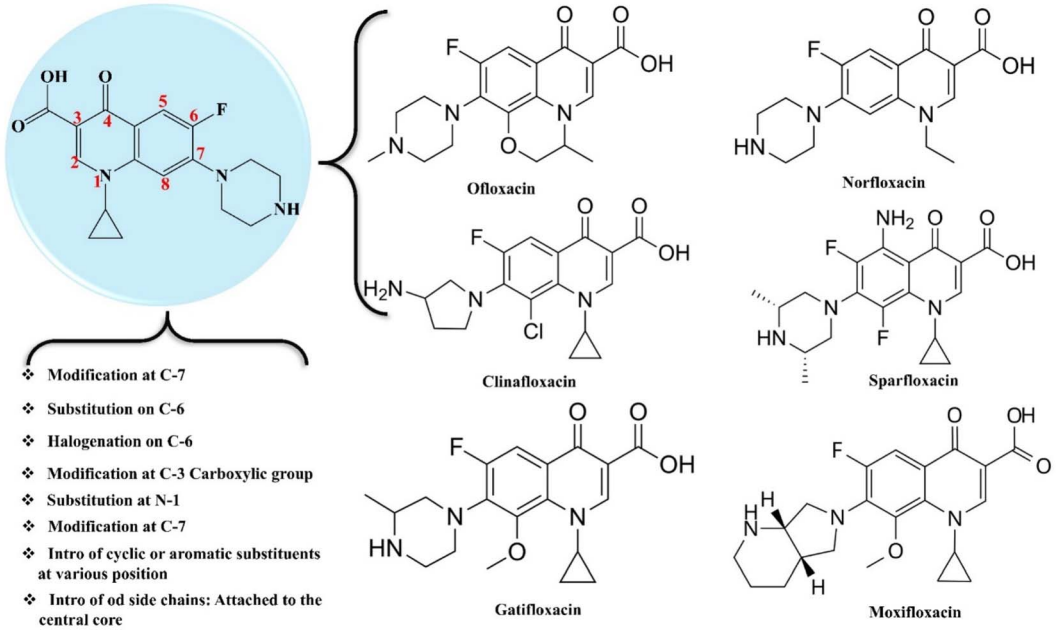

Fig. 1 Chemical structure of ciprofloxacin, possible modification in its structure with some possible derivatives.

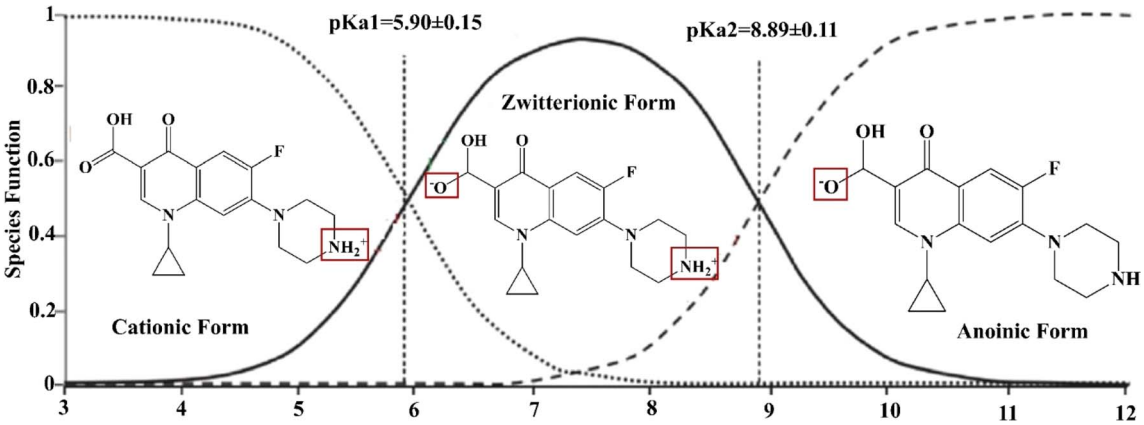

Fig. 2 Molecular structure and ionic forms of CIP as a function of pH, and pK_a values.

oxidation methods like ozonation or chlorination can partially degrade CIP, but they may also result in dangerous transformation products like halogenated byproducts, which could pose additional risks to human health and the environment.[25,26] Despite having high removal efficiencies, membrane-based technologies like reverse osmosis and nanofiltration suffer from membrane fouling, high operating costs, and frequent replacement.[27,28] Furthermore, none of these conventional techniques can guarantee that CIP is completely broken down into nontoxic end products primarily CO_2 and H_2O so residual active compounds or metabolites may still enter natural water bodies. These disadvantages highlight the urgent need for innovative, eco-friendly, and mineralization-capable technologies that can handle both the parent compound and its dangerous intermediates, such as photocatalytic degradation.[29,30] Some of the common approaches that are used for the removal of CIPs from wastewater are illustrated in Fig. 4A–E.

2. Scope and objectives of the review

This paper will provide a complete summary of the photocatalytic degradation of CIP with an emphasis on degradation pathways, operational parameters, catalyst design strategies, and degradation mechanisms. Special attention is paid to recent advancements in nanostructured photocatalysts and their application in solar or visible light irradiation. This review also critically examines the constraints, challenges of large-scale implementation, and potential directions for future research to support sustainable pharmaceutical wastewater treatment.

Fig. 3 Show some advantages of photocatalysis.

2.1. Ciprofloxacin as an emerging contaminant

The term "emerging contaminant" refers to recently found toxins in the environment that, while their effects are unknown, offer a significant risk of harm[35] as some are illustrated in Fig. 5. Pharmaceuticals are increasingly being studied as potential pollutants in water and wastewater. Pharmaceuticals enter water sources through a variety of routes, including home wastewater, hospital effluents, and agricultural runoff, damaging freshwater systems.[36] Antibiotics are a type of drug that is widely used globally to treat bacterial infections in humans, animals, and plants. They are used to treat bacterial and fungal infections in both humans and animals.[37] Ciprofloxacin (CIP) is a common second-generation fluoroquinolone antibiotic used to treat a wide range of bacterial infections in both humans and animals.[38] It is a synthetic antibiotic that operates by blocking the bacterial DNA gyrase and topoisomerase IV enzymes, which are required for DNA replication and bacterial cell division.[39] Ciprofloxacin is increasingly being categorized as a Contaminant of Emerging Concern (CEC) despite its high efficacy due to its prolonged use and

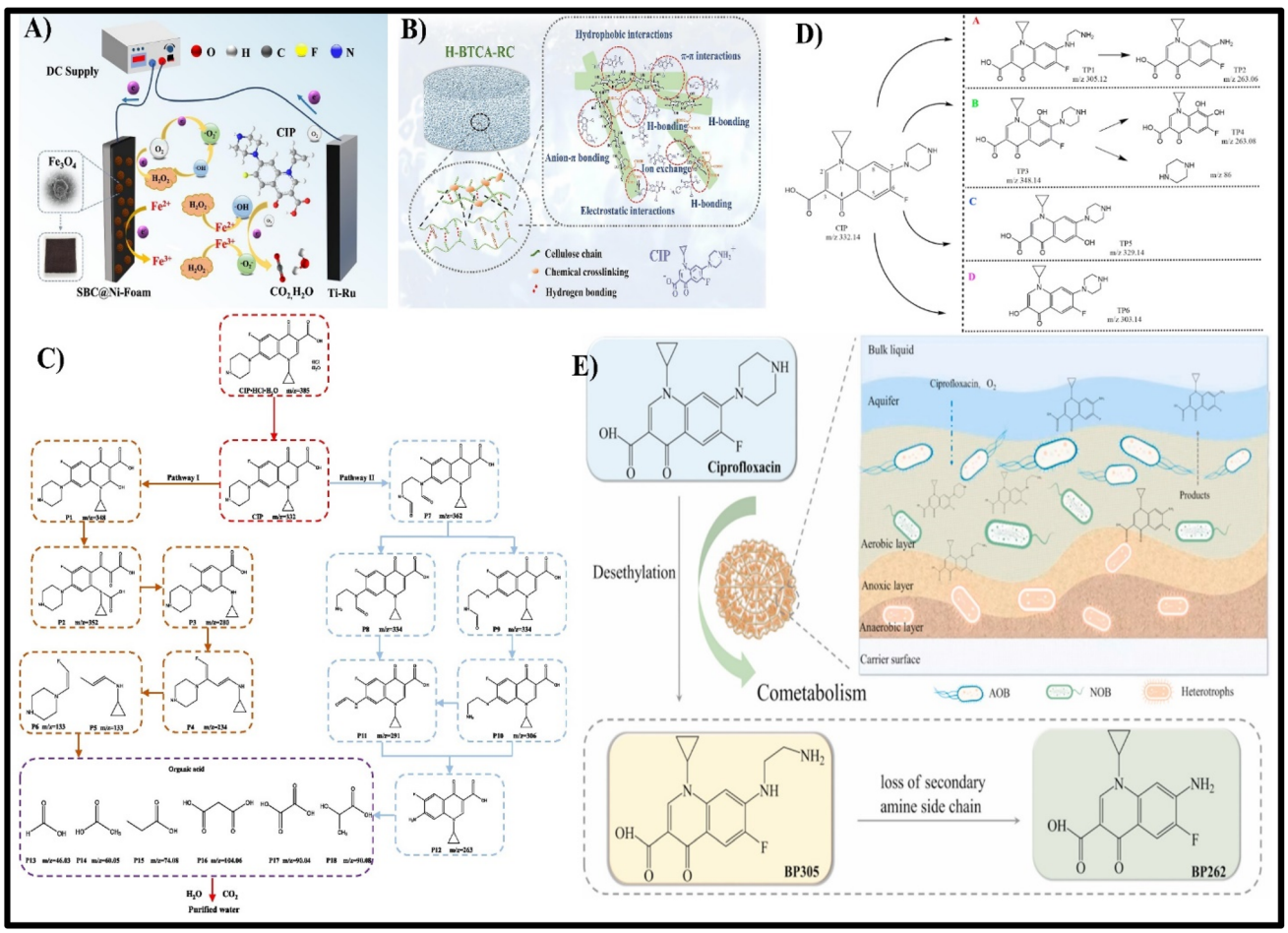

Fig. 4 Some common approaches for the removal of CIPs (A) electro-Fenton degradation pathway reproduced with permission from ref. 31 Copyright 2024, Elsevier. (B) Adsorption adopted with permission from ref. 32 Copyright 2025, Elsevier. (C) Hybrid Bio-electric degradation mechanism & (D) biodegradation of CIP in sulfate-reducing bacteria (SRB) mechanism adopted with permission from ref. 33 Copyright 2018, Elsevier. (E) Biodegradation mechanisms and pathways of ciprofloxacin retracted with permission[34] Copyright 2023, Elsevier.

perseverance, incomplete metabolism in humans and animals, and especially low biodegradability in wastewater treatment systems.[40] Significant amounts of administered ciprofloxacin are either eliminated unchanged or as active metabolites, and they find their way into the aquatic environment through municipal sewage, livestock runoff, hospital discharges, and pharmaceutical manufacturing effluents.[41,42] These pathways make CIP a pseudo-persistent compound in natural ecosystems, despite its intermittent input. According to the European Environment Agency (EEA) and the United States Geological Survey (USGS), pharmaceuticals such as ciprofloxacin are commonly found in sediments, groundwater, and surface water because they are not completely removed by traditional wastewater treatment plants (WWTPs).[43] Both human health and a variety of other organisms are at risk from ciprofloxacin residues in aquatic environments. The presence of ciprofloxacin can induce physicochemical changes that reduce the ability of high-surface-area soil components—such as clay minerals and metal oxides—to control the mobility and bioavailability of nutrients and other contaminants, thereby negatively affecting water quality.[44] Furthermore, native bacterial populations may experience chromosomal mutations because of environmental exposure to ciprofloxacin, which could lead to the emergence of antibiotic-resistant strains. Higher dosages of ciprofloxacin may therefore be needed to treat infections, and in extreme circumstances, treatment may become ineffective, raising serious public health concerns.[45] Fig. 6A1 and A2, summarized the sources and health effects of CIPs.[6]

2.1.1. Advanced oxidation processes (AOPs). An advanced oxidation processes (AOPs), processes depend on the production of extremely reactive free radicals that can oxidize and degrade organic pollutants, such as hydroxyl and singlet oxygen species. Fig. 7 represents the categories of AOPs in terms of their main activation method. AOPs like ozonation (O_3), UV/H_2O_2, Fenton process (Fe^{2+}/H_2O_2), and photo-Fenton process (Fe^{2+}/H_2O_2/UV) are most common.[46] These techniques rely on the production of extremely reactive hydroxyl radicals, which can break down recently discovered pollutants with low biodegradability and high chemical stability. When it comes to encouraging the full mineralization of pollutants into inorganic compounds, water, and CO_2, AOPs are highly effective.[47,48] The variety of AOPs includes photocatalysis (photo-Fenton reactions, UV/TiO_2), chemical oxidation processes (Fe^{2+}/H_2O_2, H_2O_2/O_3, O_3), and photochemical processes (H_2O_2/UV, O_3/UV), all of which generate OH˙ radicals.[49] The degradation pathway of CIP entails numerous key reactions, together with alterations of the piperazinyl ring, oxidation of the quinolone structure that leads to defluorination and hydroxyl substitution, and oxidative assault at the cyclopropyl group that in the end reasons ring cleavage.[50,51] Although advanced oxidation techniques by myself may additionally display confined efficiency, their performance may be drastically more desirable *via* the incorporation of chemical components along with persulfate, nanoparticles, and catalytic materials.[52,53] Nevertheless, AOPs normally yield high CIP degradation efficiencies through producing surprisingly reactive oxygen species, especially hydroxyl radicals. Advanced oxidation and discount approaches employ hydroxyl radicals (˙OH) as strong oxidants and hydrated electrons or hydrogen atoms (H˙) as decreasing agents to eliminate CIP from consuming water and wastewater.[54,55] Fig. 8 summarized general pathways of some AOPs for CIPs degradation.

AOPs are effective techniques for breaking down CIP because they use reactive species, particularly hydroxyl radicals, to convert pollutants into non-toxic byproducts. Ozonation, UV/

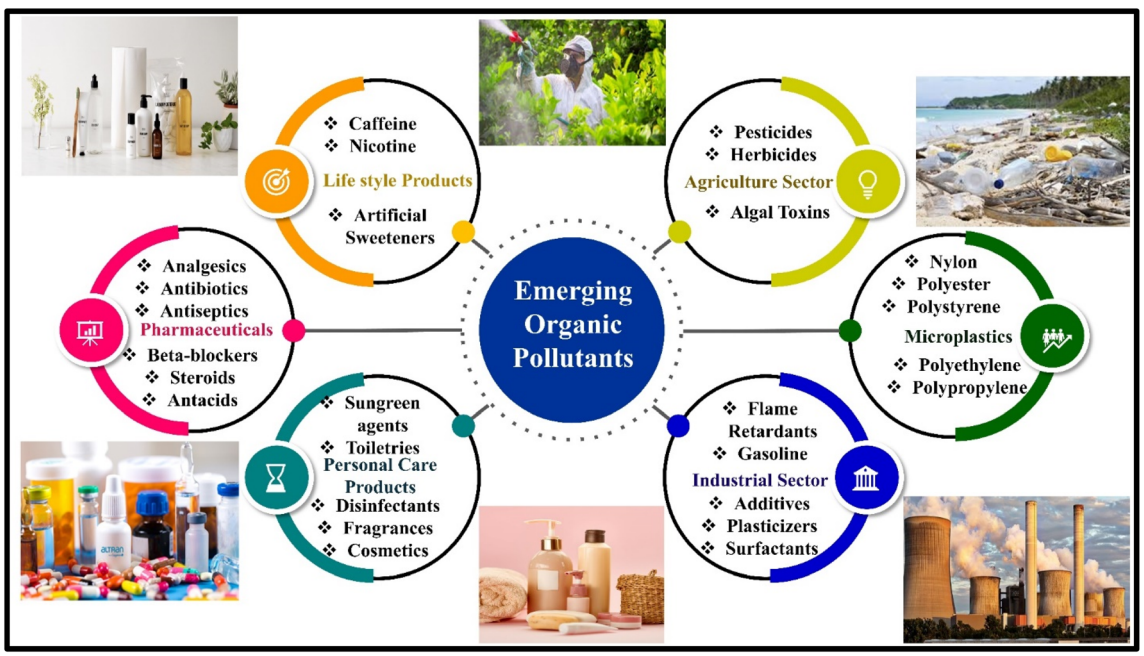

Fig. 5 Summary of some emerging organic pollutants.

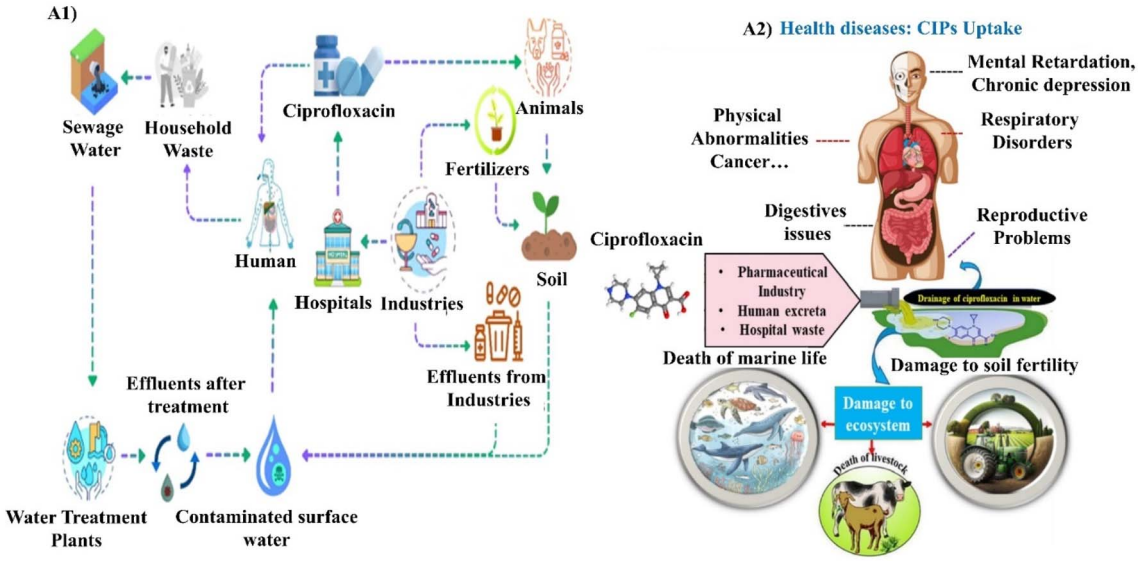

Fig. 6 (A1) Sources of CIPs. (A2) Health effects of CIPs.

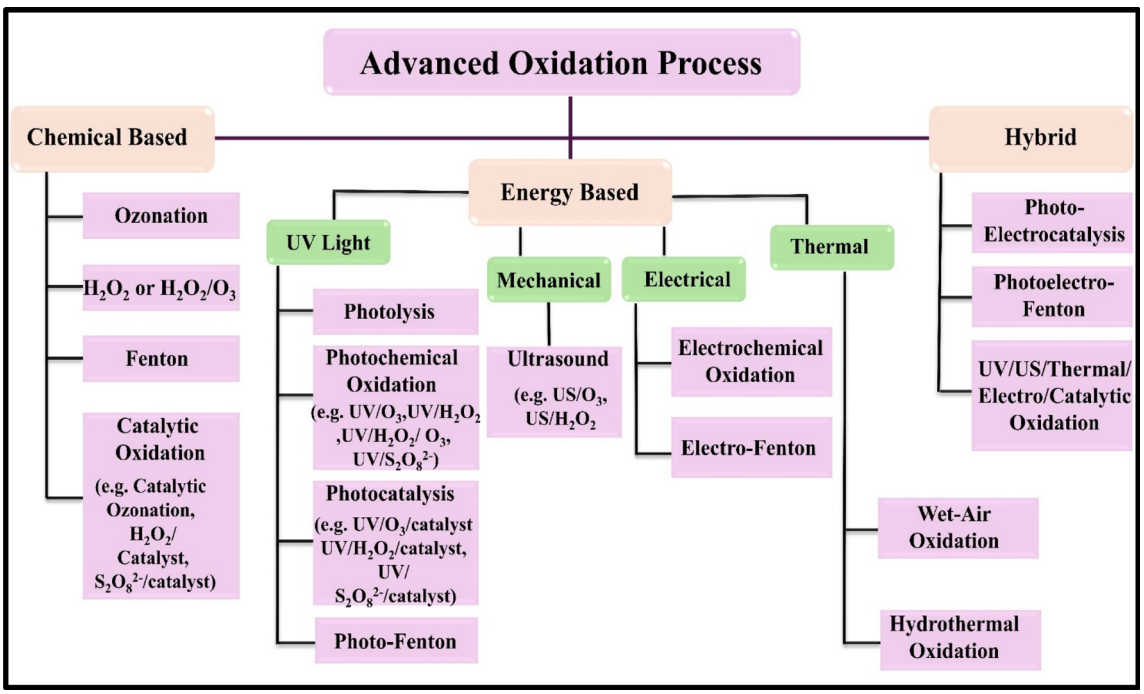

Fig. 7 Generation of oxidative radicals by AOPs in wastewater treatment.

H_2O_2, Fenton, and photo-Fenton are common methods that are frequently improved with catalysts such as layered double hydroxides or nanoparticles.[23,56] Despite their high efficiency, these processes usually require acidic conditions, which raises the cost and complexity of operations. Furthermore, certain pathways may produce hazardous byproducts, and their scalability and economic feasibility may be constrained by their high energy requirements and requirement for precise pH control.

2.2. Photocatalysis

Photocatalysis is an adjunct to conventional techniques such as membrane filtration, adsorption processes, and precipitation. This approach may be carried out as a very last step in water treatment and is in particular effective while CIP concentrations are low.[57] Through the motion of reactive species such as $OH^{\bullet}$ and/or $O_2^{\bullet}$, the method targets to absolutely mineralize organic pollution into CO_2, H_2O, and inorganic byproducts.[58] Fig. 9A, represented the detail mechanism of photocatalysis, that how it

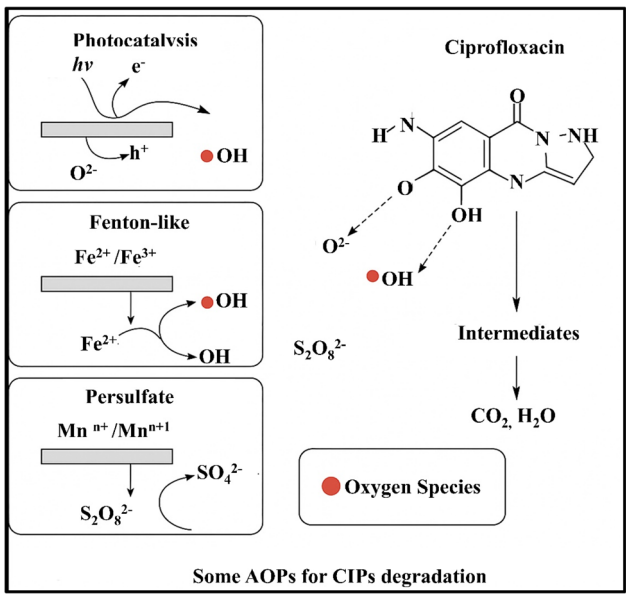

Fig. 8 Represent general pathways of some AOPs for CIPs degradation.

works while Fig. 9B demonstrated the generalized mechanism of mechanism for creation of ROS and pollutants degradation. Antibiotics like ciprofloxacin (CIP) and other organic pollutants can be transformed by these reactions into innocuous byproducts like CO_2, H_2O, and inorganic ions.[59] The system is initiated when mild energy is same to or greater than the bandgap of a photocatalyst—which includes metal oxides absorbed. Fig. 10, summarized some metal oxide recently used for CIPs degradation[60] while Fig. 11 illustrated various pathway for obtaining these oxides.[61] This strength excites an electron (e^-) from the valence band (VB) to the conduction band (CB), leaving in the back of a hollow (h^+) inside the VB.[62] The formation of these electron–hole pairs is essential for triggering redox reactions at the catalyst surface. Once they migrate to the surface, the photogenerated electrons and holes participate in chemical reactions with adsorbed species: the holes oxidize water or hydroxide ions to generate hydroxyl radicals (˙OH), even as the electrons lessen molecular oxygen to form reactive oxygen species, along with superoxide anions (O_2^-). Depending on the use, these extremely reactive species can destroy microorganisms, split water to create hydrogen, or break down organic pollutants.[63,64] However, its effectiveness is constrained at better antibiotic concentrations, wherein excessive pollutant stages can hinder light penetration and decrease touch with the catalyst surface, thereby slowing the reaction.[65] There are two categories of photocatalysis: heterogeneous and homogeneous as they are presented in Fig. 12. Heterogeneous photocatalysis relies on surface-mediated redox reactions on solid semiconductors, whereas homogeneous photocatalysis proceeds *via* dissolved photoactive species that generate reactive oxygen species directly in the reaction medium.[66] Heterogeneous photocatalysis is more frequently researched and used for photodegradation of CIPs. Various photocatalyst heterojunction interface are represented in Fig. 13.[67] Rapid electron–hole pair recombination limited visible light absorption (since many conventional photocatalysts only react to UV light), and stability problems like photo corrosion are some of the obstacles that photocatalysis must overcome despite its potential.[68]

Researchers are looking at a number of approaches to overcome these constraints, such as creating heterojunctions to improve charge separation, doping with metal or non-metal elements to narrow the band gap, and creating plasmonic photocatalysts that improve light absorption through surface

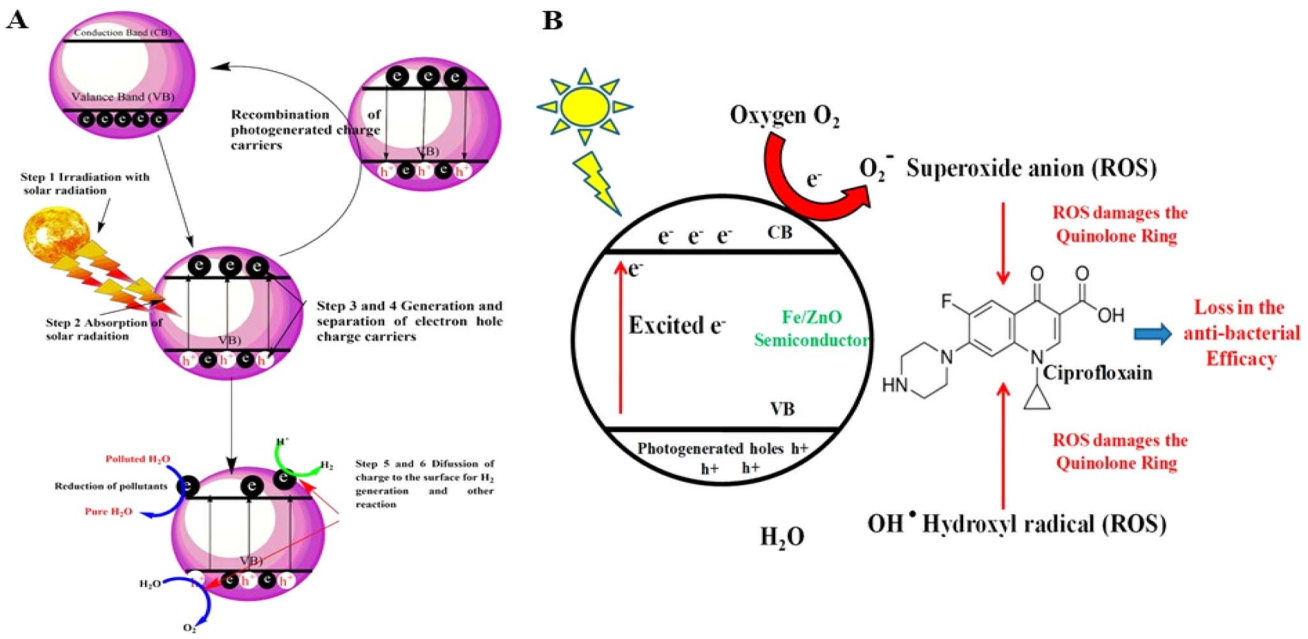

Fig. 9 (A) Detailed mechanism of photocatalysis. (B) Pictorial presentation of photodegradation of pollutants.

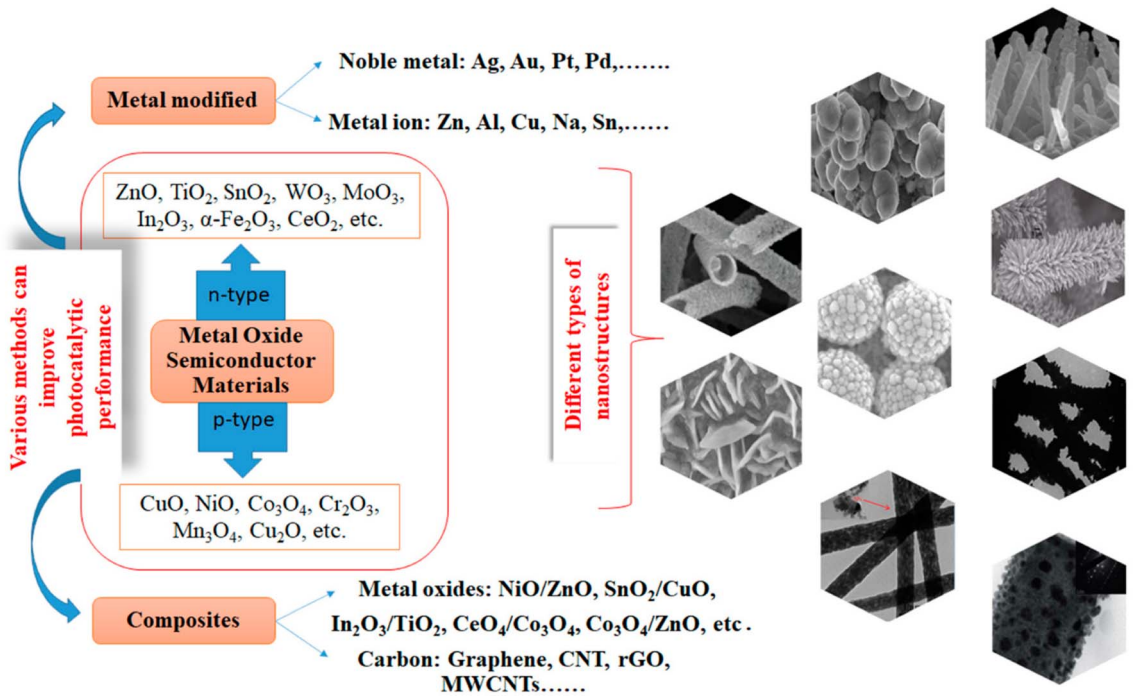

Fig. 10 Various metal oxides for photocatalysis of CIPs reprinted with permission from ref. 60 Copyright 2023, mdpi.

plasmon resonance.[69,70] All things considered, photocatalysis is still developing and presents viable options for sustainable energy generation and environmental cleanup. To overcome present constraints and make it possible for photocatalytic technologies to be used on a large scale, advances in material science and nanotechnology are essential.

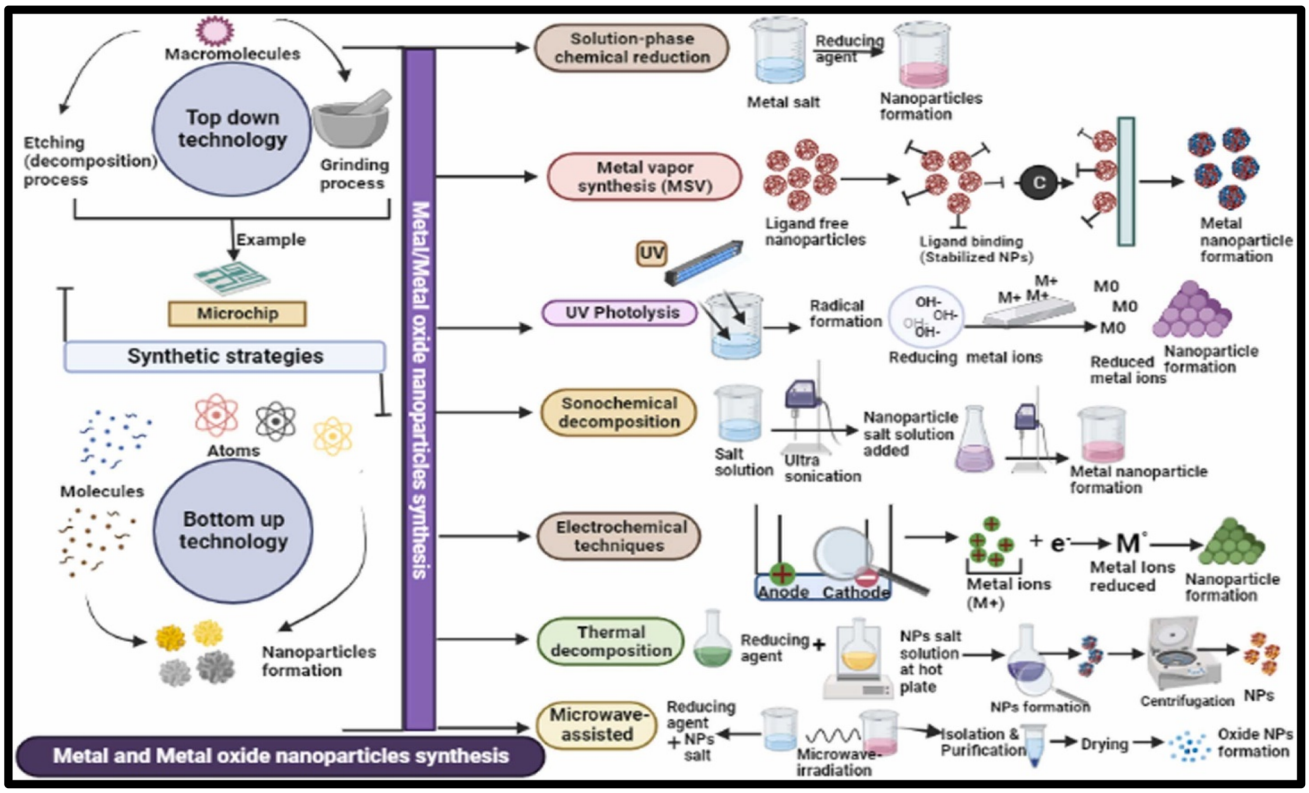

Fig. 11 Methods for synthesizing these catalysts modified with permission from ref. 61 Copyright 2022, Elsevier.

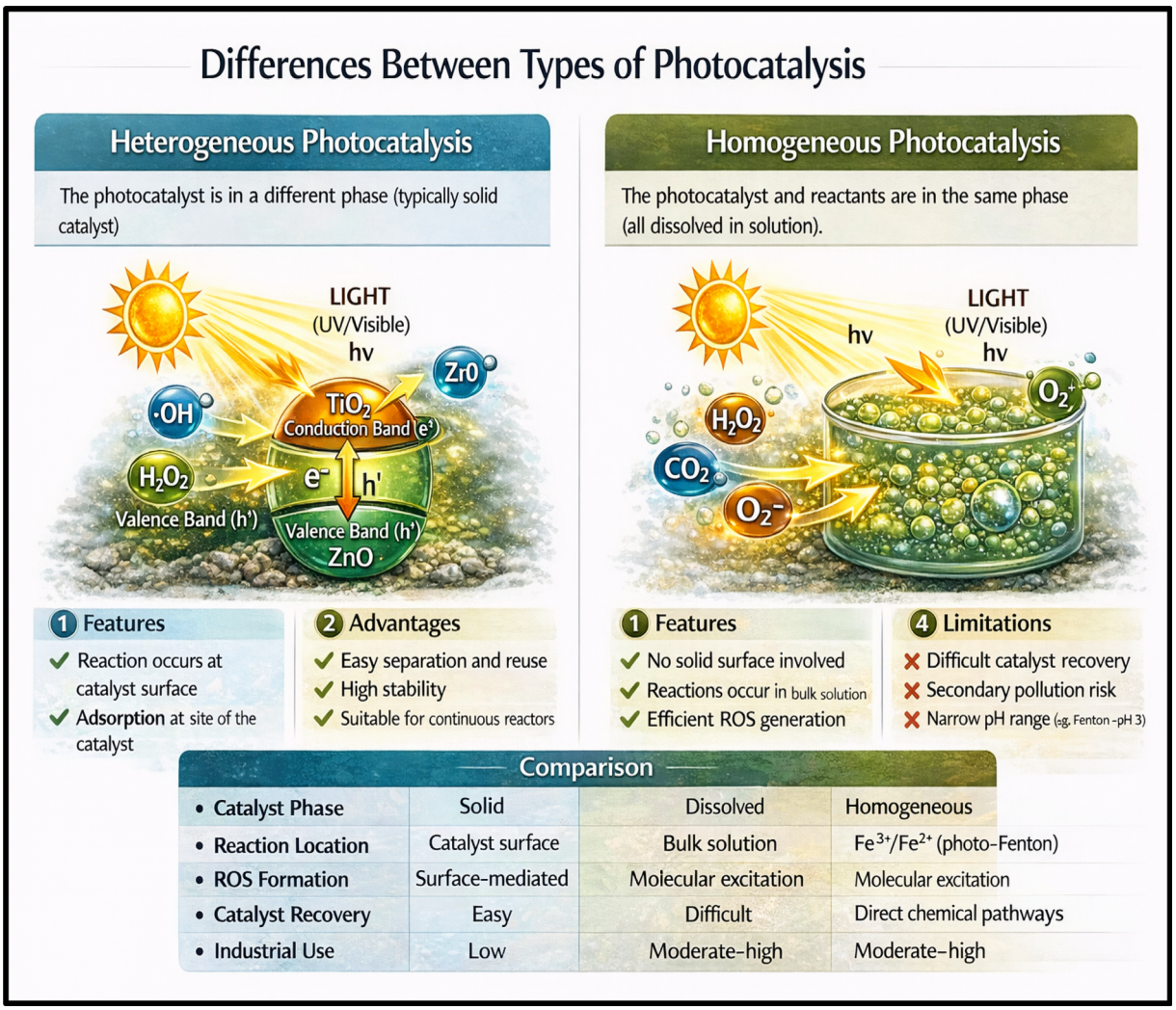

Fig. 12 Difference b/w hetero- and homogenous photocatalysis.

2.2.1. Emerging trends in photocatalytic materials. Photocatalytic materials have developed quickly in recent year to improve light absorption and charge separation efficiency, and surface reactivity for the degradation of persistent pollutants such as ciprofloxacin (CIP).[71] Traditional photocatalysts like ZnO and TiO_2 are still being studied in great detail due to their stability and lack of toxicity,.[72] Fig. 14A shows general photo-degradation mechanism followed by ZnO photocatalyst.[73] Similarly, Fig. 14B illustrates a schematic of the degradation of contaminants by forming photo-induced charge carrier electrons/holes (e^-/h^+) on the TiO_2 surface. Also, Fig. 14C shows how photodegradation occur on TiO_2 photocatalyst.[74] But their use in visible light is limited by their wide band gaps. Some serious modification strategies are implemented to overcome these limitations, as some are listed in Fig. 14D.[75] One modification strategy that has been developed to overcome these limitations is doping with metal or non-metal ions (*e.g.*, Fe, Ag, N, or C) to tune band gap energy and extend photo-response into the visible region[76,77] as some are shown in Fig. 15A.[78] It has also been shown that heterojunction engineering, such as coupling TiO_2 with g-C_3N_4, Cds, or reduced graphene oxide (rGO), can improve charge carrier separation and reduce recombination rates.[79] 2D nanostructures (like graphitic carbon nitride nanosheets and MXenes) have further increased catalytic activity by providing large surface areas and a large number of reactive sites.[80] Additionally, plasmonic photocatalysts that use noble metals (Au, Ag) utilize localized surface plasmon resonance (LSPR) effects to improve visible light harvesting, generalized mechanism are pictorially represented in Fig. 15B.[81] Recent studies have also focused on Z-scheme systems and MOF-derived photocatalysts, which combine a high redox potential with a strong charge separation ability. Fig. 16A depicted application of MOF as photocatalyst[82] while Fig. 16B demonstrating CIP photodegradation *via* MOF based photocatalyst (BiOX/GaMOF).[63] These advancements demonstrate a clear trend toward multi-component, visible, light-active, environmentally safe photocatalysts that are intended to effectively degrade antibiotics.

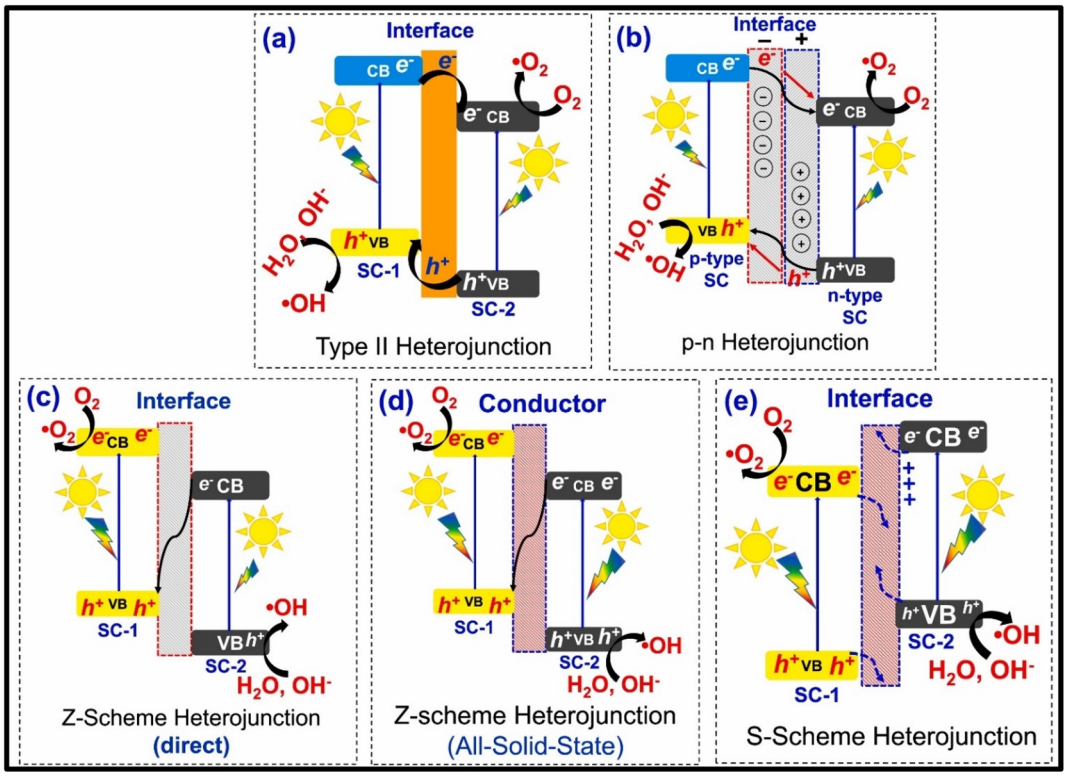

Fig. 13 Various photocatalyst heterojunction interfaces: (a) type-II heterojunction, (b) P–N heterojunction, (c) direct Z-scheme heterojunction, (d) all-solid-state Z-scheme heterojunction, and (e) S-scheme heterojunction reproduced with permission from ref. 67 Copyright 2024, Elsevier.

3. Photocatalyst for ciprofloxacin degradation

A common fluoroquinolone antibiotic, ciprofloxacin (CIP), has been successfully and sustainably removed from aquatic environments by photocatalytic degradation. Over the past decade, numerous semiconducting substances were advanced and modified to decorate the photocatalytic degradation performance of CIP below both visible and UV light. These materials' structure, composition, light-absorbing ability, and charge carrier dynamics all affect how well they work in photocatalytic applications.[83] Some common categories of catalysts are presented in Fig. 17.

3.1. TiO_2-based photocatalysts

Titanium dioxide (TiO_2) remains the most considerably studied photocatalyst for CIP degradation due to its strong oxidative electricity, low value, non-toxicity, and extremely good chemical stability. The proposed degradation mechanism for CIPs followed by TiO_2 photocatalyst are illustrated in eqn (1)–(8).[84,85] Mechanistically presented in Fig. 18A.[86] However, its wide bandgap (about 3.2 eV for anatase) limits its pastime to the ultraviolet (UV) location, which represents simplest a small fraction of the solar spectrum.[87] Scientists have used a variety of methods, including heterojunction formation, surface sensitization, and metal and non-metal doping, to drastically change TiO_2 in order to overcome this limitation. Fig. 18B, demonstrated the visual representation of bandgap with pure TiO_2, with metal and non-metal doped.[88] For example, nitrogen-doped TiO_2 has demonstrated notably enhanced activity under visible light by narrowing the bandgap.[89] Moreover, combining TiO_2 with different semiconductors or carbon-based materials, together with graphene oxide or graphitic carbon nitride (g-C_3N_4), enhances price separation and broadens its light absorption range. Fig. 18C demonstrated CIPs degradation *via* BGCN-TiO_2.[90]

$$TiO_2 + h\nu \rightarrow h^+ + e^- \quad (1)$$

$$O_2 + e^- \rightarrow O_2^{\bullet -} \quad (2)$$

$$H_2O + h^+ \rightarrow H^+ + OH^\bullet \quad (3)$$

$$OH + h^+ \rightarrow OH^\bullet \quad (4)$$

$$2O_2^{\bullet -} + 2H^+ \rightarrow H_2O_2 + O_2 \quad (5)$$

$$OH^\bullet + OH^\bullet \rightarrow H_2O_2 \quad (6)$$

$$H_2O_2 + O_2^{\bullet -} \rightarrow OH^\bullet + OH^- + O_2 \quad (7)$$

$$CIPs + O_2^{\bullet -} + OH^\bullet \rightarrow CO_2 + O_2 + \text{by-product} \quad (8)$$

Titanium dioxide (TiO_2) has tested considerable efficacy in ciprofloxacin (CIP) degradation, achieving a 92.91%

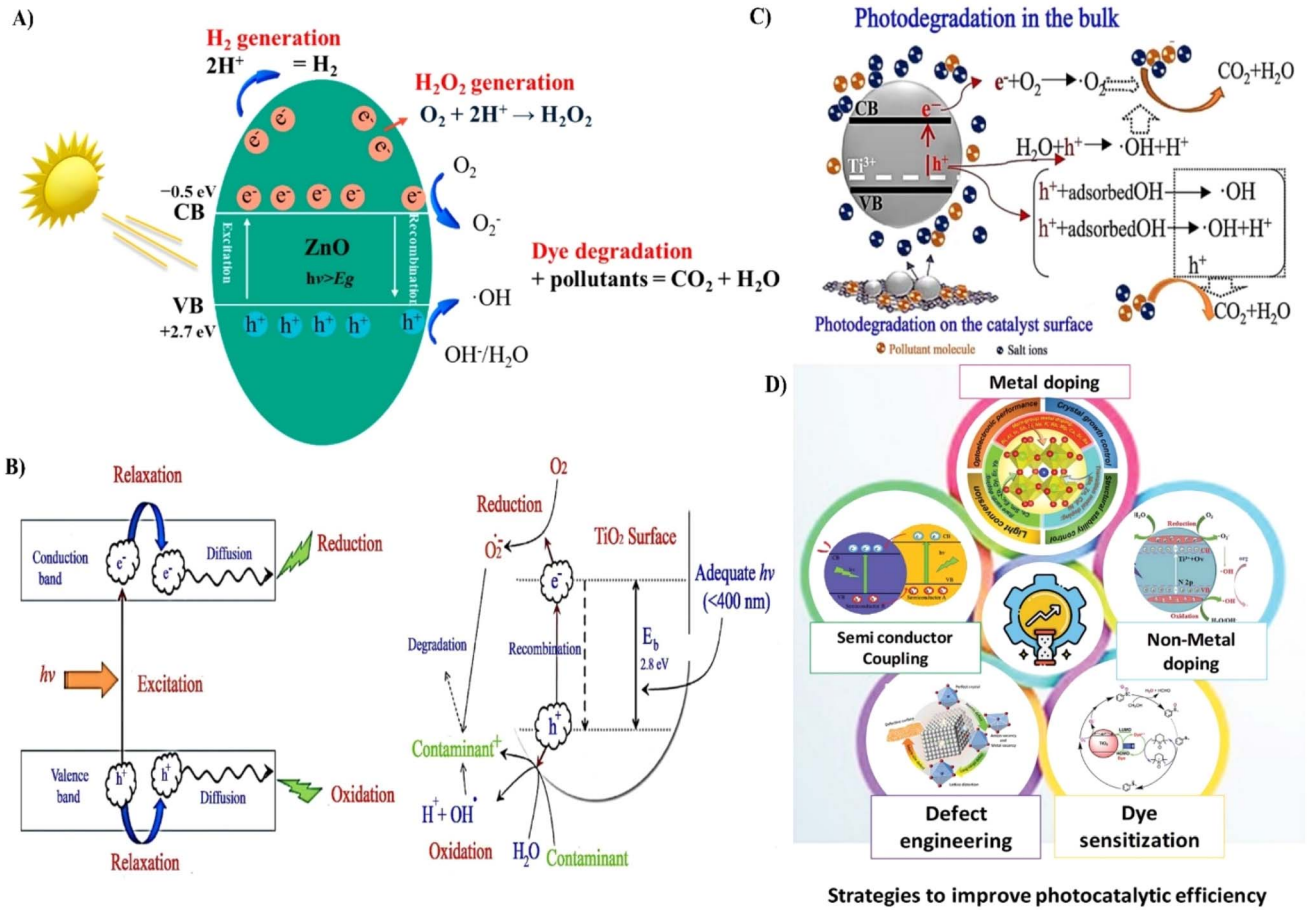

Fig. 14 (A) Illustration of photocatalytic mechanism followed by ZnO photocatalyst adopted with permission from ref. 73 Copyright 2025, mdpi. (B) Creation of photo-induced charge carrier e^-/h^+ on the TiO_2 surface & (C) illustration of photodegradation on TiO_2 surface adopted with permission from ref. 74 Copyright 2024, mdpi. (D) Techniques for improving photocatalytic efficiency reproduced with permission from ref. 75 Copyright 2025, Taylor & Francis.

elimination efficiency and following pseudo-2nd order kinetics with a price steady (k) of 0.056 min^{-1} after 240 minutes of irradiation.[91] Buu *et al.* reported 99.7% CIP elimination in just one hundred mins under seen mild the use of a TiO_2–ZnO heterojunction with a Z-scheme configuration incorporated into an oxygen-doped graphitic carbon nitride (g-C_3N_4) matrix, following pseudo-first-order kinetics with a fee steady of 0.04796 min^{-1}.[92] In pursuit of developing S-scheme photocatalysts for water purification, heterojunction composites were designed, including Fe-based metal–organic framework (MIL-101(Fe))/BiOBr and Bi_2WO_6/C_3N_4/carbon fiber systems.[93,94] They improved the photocatalytic performance of TiO_2/AgBr/Ag by designing S-scheme heterojunctions, achieving an excellent removal efficiency of 86.18% following pseudo-first-order kinetics. In addition, they developed a ternary film composed of rutile–anatase TiO_2 (B-TiO_2), bismuth sulfide, and photonic crystals (B-TiO_2/Bi_2S_3/PCs). This system significantly outperformed pristine B-TiO_2 in ciprofloxacin (CIP) degradation, attaining a removal efficiency of 72.79% with outstanding reusability.[95] It was demonstrated that the $TiO_2/NiFe_2O_4$@-MWCNTs nanocomposite is a highly efficient and sustainable photocatalyst, achieving up to 97.2% degradation of ciprofloxacin (CIP) under pseudo-first-order kinetics. Notably, its photocatalytic performance decreased by less than 3.2% after four consecutive cycles, indicating excellent stability and long-term applicability for water purification.[132] Surface change through dye sensitization—the usage of herbal or artificial dyes to create catalysts responsive to visible or sun mild—is another environmentally pleasant approach.[96] Carbon quantum dots embellished on nitrogen- and copper-co-doped TiO_2 (NCuTCQD) have shown superior overall performance, attaining entire (100%) CIP degradation at a wonderful charge with minimum loss of activity after six cycles [97] outperforming traditional TiO_2-primarily based photocatalysts. Table 1 illustrated CIPs degradation *via* TiO_2 based photocatalyst.

3.2. ZnO-based photocatalysts

Zinc oxide (ZnO) remains a highly valued photocatalyst for CIPs degradation (eqn (9)–(18)) due to its low cost, high electron mobility, and short-term photostability.[109] However, ZnO's wide bandgap (~3.3 eV) restricts its activation to UV light, limiting its use under solar irradiation.[110] Moreover, photocorrosion and the rapid recombination of photogenerated e^-/h^+ pairs reduce

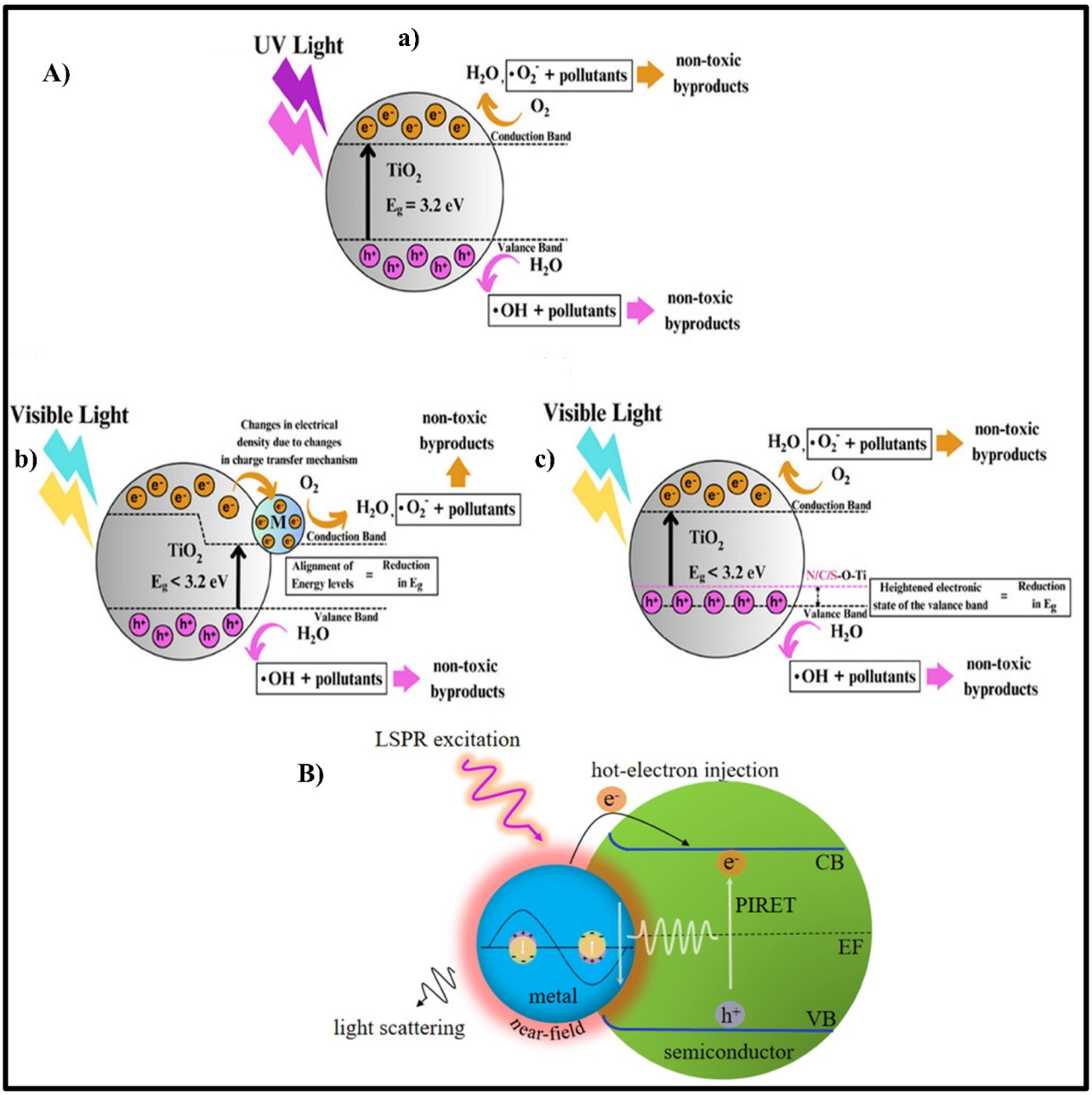

Fig. 15 (A) Illustration of the photocatalytic mechanism of (a) pure-TiO_2, (b) metal-doped, and (c) nonmetal-doped TiO_2 reproduced with permission from ref. 78 Copyright 2025, Viley-VcH. (B) Mechanism diagram for plasmonic metal–semiconductor photocatalysis reproduced with permission from ref. 81 Copyright 2024, Royal Society of Chemistry.

its long-term applicability and efficiency.[111] To address these limitations, various modification strategies—such as metal/non-metal doping, co-doping, composite formation, and sensitization techniques—have been explored to improve ZnO's visible-light responsiveness and suppress charge recombination. hence strategies are summarized in Fig. 19A–D.[112] With Fig. 19A and B demonstrating the photodegradation of CIPs by doped Cu-ZnO/g-C_3N_4 (ref. 113) and Ag-doped ZnO (ZnO/Ag(3))[114] respectively (Fig. 20).

$$ZnO + h\nu \rightarrow ZnO\ (h^+ + e^-) \quad (9)$$

$$e^- + O_2 \rightarrow O_2^{\bullet -} \quad (10)$$

$$O_2^{\bullet -} + H^+ \rightarrow HO_2^{\bullet} \quad (11)$$

$$HO_2^{\bullet} + HO_2^{\bullet} \rightarrow H_2O_2 + O_2 \quad (12)$$

$$H_2O_2 + HO_2^{\bullet} \rightarrow OH^{\bullet} + OH^- + O_2 \quad (13)$$

$$H_2O_2 + h\nu \rightarrow 2OH^{\bullet} \quad (14)$$

$$H_2O_2 + e^- \rightarrow OH^{\bullet} + OH^- \quad (15)$$

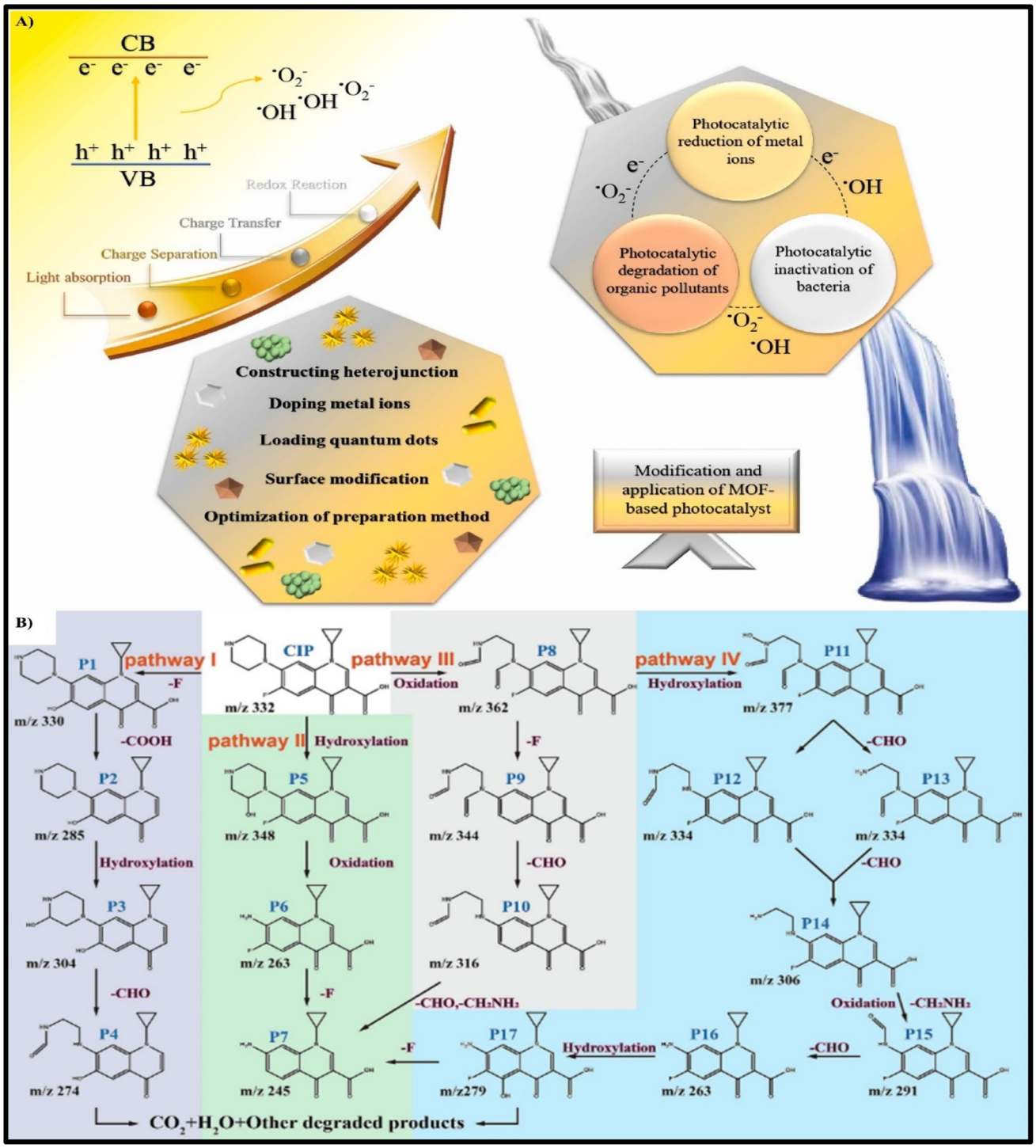

Fig. 16 (A) MOF as photocatalyst reprinted with permission from ref. 82 Copyright 2024, Heliyon. (B) LC-MS of photodegradation of CIP using BiOX/GaMOF photocatalyst adopted with permission from ref. 63 Copyright 2025, Elsevier.

$$H_2O + h^+ \rightarrow OH^{\cdot} + H^+ \quad (16)$$

$$OH^- + h^+ \rightarrow OH^{\cdot} \quad (17)$$

$$OH^{\cdot} + CIPs \rightarrow \text{intermediates} \rightarrow CO_2 + H_2O \quad (18)$$

For instance, ZnO and iron-doped ZnO photocatalysts with doping concentrations of 0.1% and 0.2% have been synthesized using the sol–gel method and evaluated for ciprofloxacin degradation. The 0.2% Fe-doped ZnO exhibited the highest degradation performance of 90.49%. Kinetic analysis revealed that the response observed pseudo-first-order conduct, confirming the enhanced catalytic performance facilitated through

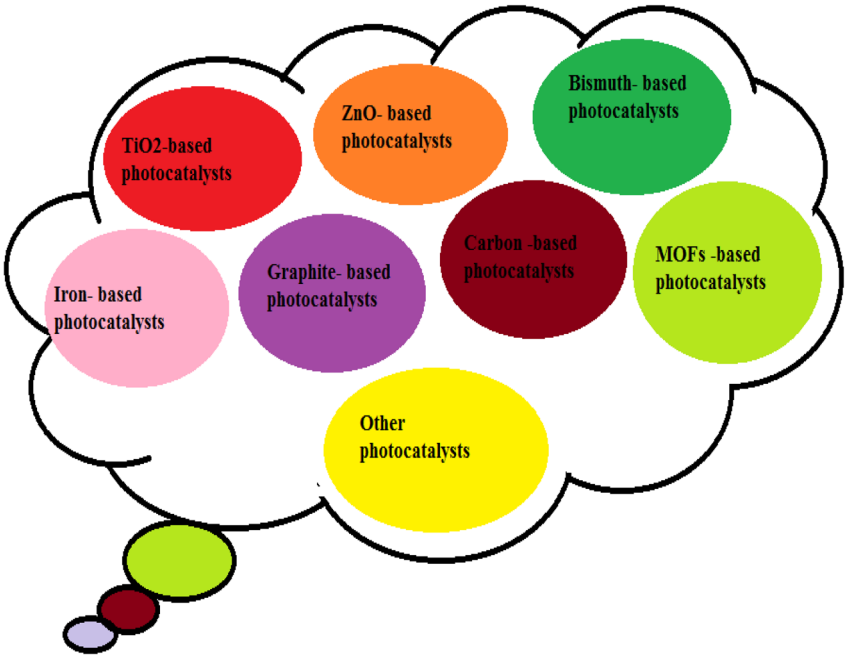

Fig. 17 Some common categories of photocatalysts.

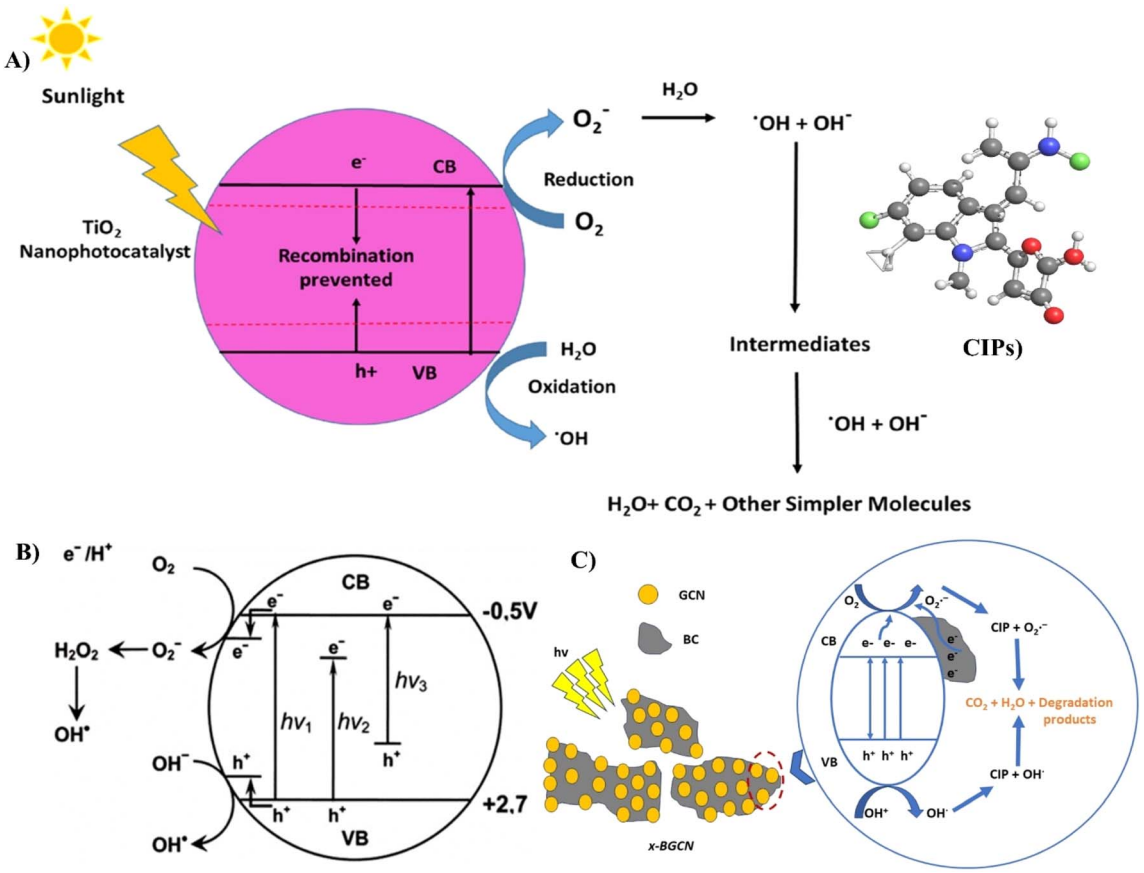

Fig. 18 (A) Photocatalytic degradation mechanism of ciprofloxacin and amoxicillin using TiO_2 photocatalyst under sunlight, reused with permission from ref. 86 Copyright 2024, American Chemical Society. (B) Illustration of photocatalysis process of TiO_2. $h\nu_1$: pristine TiO_2; $h\nu_2$: metal doped TiO_2; and $h\nu_3$: nonmetal doped TiO_2 retaken with permission from ref. 88 Copyright 2022, mdpi. (C) Suggested degradation mechanism of removal of CIP micropollutant *via* BGCN-TiO_2 adopted with permission from ref. 90, Copyright 2025, IOPscience.

Table 1 TiO_2 based photocatalysts for ciprofloxacin degradation concentration efficiency and kinetic parameters

S/n	Catalyst	Dosage ($g\ L^{-1}$)	Light source	Concentration of CIPs ($mg\ L^{-1}$)	Kinetics model	Rate constant (min^{-1})	Time (min)	Efficiency (%)	Ref.
1	TiO_2 powder	0.1	16 W UV lamp	20	Pseudo 1st order	0.0063	120	57	98
2	TiO_2/montmorillonite	0.1	16 W UV lamp	20	Pseudo 1st order	0.0069	120	62	98
3	TiO_2 powder	0.5	UV (485 $\mu W\ cm^{-2}$) lamp	45.3 μM	Pseudo 1st order	0.137	40	—	99
4	TiO_2/montmorillonite	0.04	UV lamp	20	—	—	30	90	100
5	TiO_2 powder	0.5	UV (389 $\mu W\ cm^{-2}$) lamp	45.3 μM	Pseudo 1st order	163	40	—	99
6	g-C_3N_4/TiO_2 powder	1	150 W tungsten lamp	10	—	—	60	95	101
7	TiO_2 powder	1	HQI-T 250/daylight	50	Pseudo 1st order	0.04	120	—	102
8	TiO_2 immobilized on glass plates	—	15 W UV lamp	60	Pseudo 1st order	0.024	120	97	103
9	PVA assisted TiO_2/Ti film	—	300 W xenon lamp	10	Pseudo 1st order	0.0244	60	77	104
10	g-C_3N_4/TiO_2/kaolinite	2	Xenon lamp (90 $mW\ cm^{-2}$)	10	Pseudo 1st order	0.0081	240	92	105
11	N-doped TiO_2	1	400 W visible tungsten lamp	100	Pseudo 1st order	0.073	90	100	106
12	Fe_3O_4/TiO_2/C-dot	0.75	Mercury vapor lamp	20	Pseudo 1st order	0.0154	150	90	107
13	P-25 TiO_2	1	400 W tungsten lamp	100	Pseudo 1st order	0.059	180	—	106
14	P-25 TiO_2	1	Solar radiation	100	Pseudo 1st order	0.108	180	—	106
15	TiO_2 nanoparticles	1	UV lamp	300 $\mu g\ L^{-1}$	—	—	45	100	108

iron doping. This catalyst has the potential to clean contaminated wastewater, as demonstrated by researchers' effective use of it to break down ciprofloxacin in commercial samples.[115] Moreover, cobalt-doped ZnO nanoparticles showed strong CIP elimination. Furthermore, research have shown that redecorating zinc oxide nanoparticles with carbon dots substantially complements their photocatalytic performance, achieving a CIP elimination efficiency of up to 98%.[116] As previously cited, building heterojunctions is any other broadly adopted method to improve visible-light pastime and rate separation in photocatalysts. For instance, Ye *et al.* developed a Z-scheme heterojunction composed of $CaFe_2O_4$, Ag, and ZnO nanoparticles, which established stepped forward seen-light absorption and more advantageous photocatalytic efficiency.[117] Table 2. Summarizes ZnO based photocatalyst for CIPs degradation.

3.3. Bismuth-based photocatalyst

Bismuth (Bi) covers a wide range of materials, as their categories are summarized in Fig. 21.[127]

Interest has been piqued by the unique layered structures of bismuth-based photocatalysts, particularly BiOCl, $BiVO_4$, and Bi_2WO_6, which generate internal electric fields that aid in charge carrier separation. These substances work remarkably well in visible light and have been successfully used to break down several pharmaceutical contaminants, including CIP.[128,129] For example, $BiVO_4$/g-C_3N_4 nanocomposites showed over 85% degradation efficiencies after 90 minutes of exposure to visible light. Proposed photocatalytic mechanism followed by $BiVO_4$/g-C_3N_4 for CIPs is shown in Fig. 22A and B respectively.[130] Their photocatalytic activity is further enhanced by doping with metals like molybdenum (Mo) or silver (Ag), which increase electron mobility and broaden the range of light absorption. Bandgaps for various bismuth-based photocatalysts are illustrated in Fig. 22C.[131]

Since their bandgap is typically less than 3 eV, they can be used in situations where visible light is present. BBSc's photocatalytic qualities have attracted a lot of interest. For example, Hai *et al.* synthesized two bismuth oxide (BiOI) substances: BiOI-R through hydrolysis and BiOI-S through a solvothermal technique. Under seen mild, BiOI-S exhibited incredible adsorption and photocatalytic degradation overall performance for ciprofloxacin, accomplishing an outstanding elimination efficiency of 99.89%. Fig. 23A demonstrated the bandgap energy and degradation pathway for CIP by proposed material.[132] The formation of heterojunctions in bismuth-based totally photocatalysts has further greater their photocatalytic pastime. Examples encompass nitrogen-doped carbon quantum dots mixed with bismuth tungstate (NCQDs/Bi_2WO_6),[133] SiO_2/Bi_2O_3/Ag, Bi/BiOF/$Bi_2O_2CO_3$, and WS_2/BiOCl with oxygen vacancies (4-WS_2/BiOCl_OV).[134] These heterojunctions enhance photocatalytic overall performance by way of enhancing light absorption, promoting efficient fee separation, and

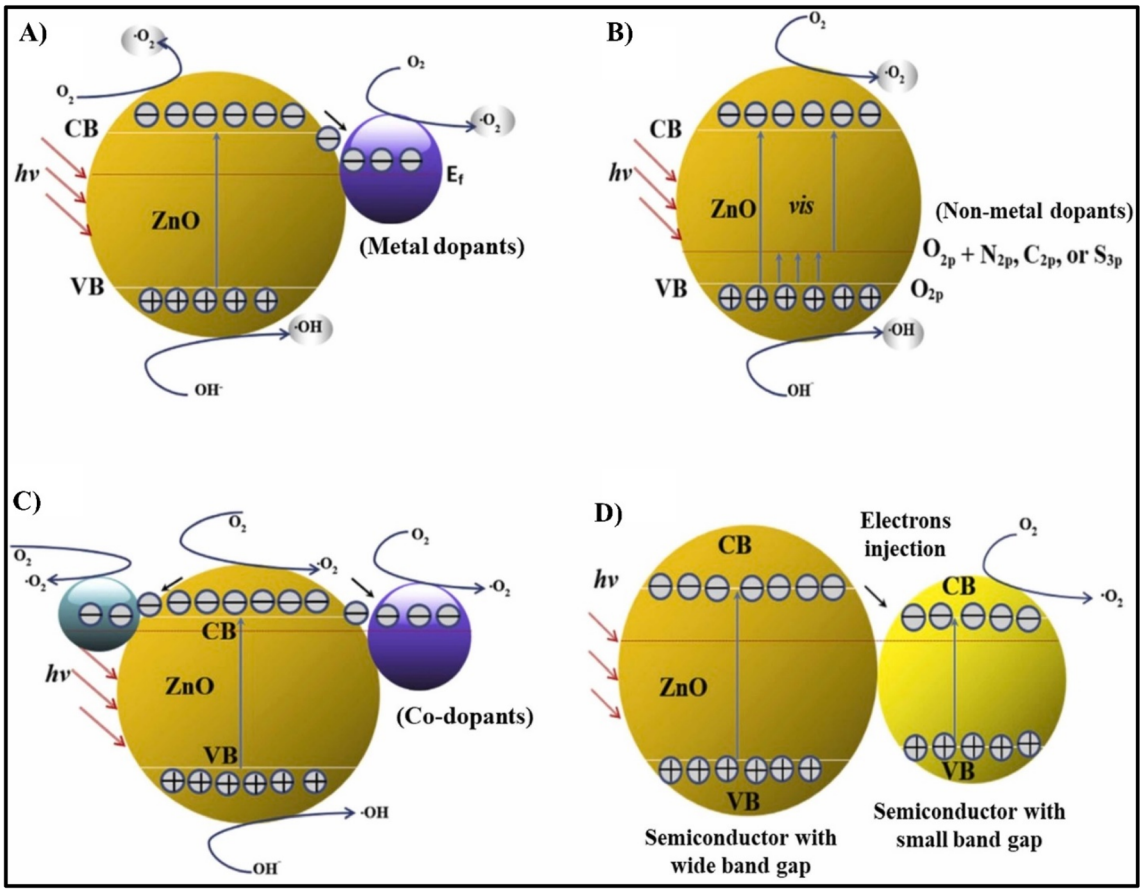

Fig. 19 The proposed photocatalytic degradation by (A) metal doping, (B) non-metal doping, (C) co-doping, and (D) coupling semiconductor on ZnO surface reproduced with permission from ref. 112 Copyright 2022, Elsevier.

strengthening redox competencies. Bismuth-based semiconductors (BBSc) with metallic doping exhibit increased photocatalytic activity.[135] Research has indicated that metal-doped BBScs, including Zn-doped BiOBr, Cu-doped Bi_2O_3, and Gd^{3+}-doped Bi_4O_5 (ref. 136) have enhanced photocatalytic performance. These metal-doped semiconductors have demonstrated better redox characteristics, more light absorption, and greater charge separation. Numerous attempts have been made to create and employ bismuth-based photocatalysts that are durable. For example, an α-Fe_2O_3–modified Bi_2WO_6 heterostructure photocatalyst was developed, which exhibited excellent photocatalytic activity and maintained stable performance even after six consecutive cycles, with no discernible loss in activity.[137] Table 3 presented Bi-based photocatalysts for ciprofloxacin degradation.

3.4. Iron based photocatalysts

Iron oxide semiconductors have proven extraordinary potential for photocatalytic programs in environmental remediation due to exceptional features.[151] As illustrated in Fig. 23B, iron oxide nanoparticles provide numerous benefits as photocatalysts. Naturally, iron oxides occur in 3 foremost paperwork: magnetite (Fe_3O_4), hematite (α-Fe_2O_3), and maghemite (γ-Fe_2O_3).[152] Among those, hematite (α-Fe_2O_3) is a crimson-colored n-type semiconductor acknowledged for its unique homes, together with an indirect bandgap of 2.1 eV, herbal abundance, low-cost synthesis, excessive chemical balance, environmental friendliness, and ease of recovery.[153]

Research has shown that editing iron-based totally photocatalysts can substantially beautify their photocatalytic overall performance. For example, researchers investigated the degradation of 10 mg L^{-1} ciprofloxacin under solar irradiation using both pristine and composite photocatalysts, including Fe_2O_3 and Ni-doped Fe_2O_3. The Ni-doped Fe_2O_3 exhibited a 42.1% enhancement in photocatalytic activity compared with the pristine material.[154] Additionally, a Ni-doped α-Fe_2O_3/g-C_3N_4 nanocomposite synthesized through an easy co-precipitation technique tested advanced pastime, reaching an 82.1% removal efficiency. This improved overall performance was attributed to improved charge separation and decreased electron–hole recombination. Heterojunction formation similarly improves the photocatalytic efficiency of iron-primarily based materials. Cai *et al.* developed a Z-scheme heterojunction composed of α-Fe_2O_3@geopolymer spheres decorated with MnO_2, accomplishing 91% degradation of 20 mg per L ciprofloxacin below visible mild. The proposed degradation pathways is depicted in Fig. 23C.[155] Table 4, summarizes CIPs degradation *via* Fe-photocatalyst.

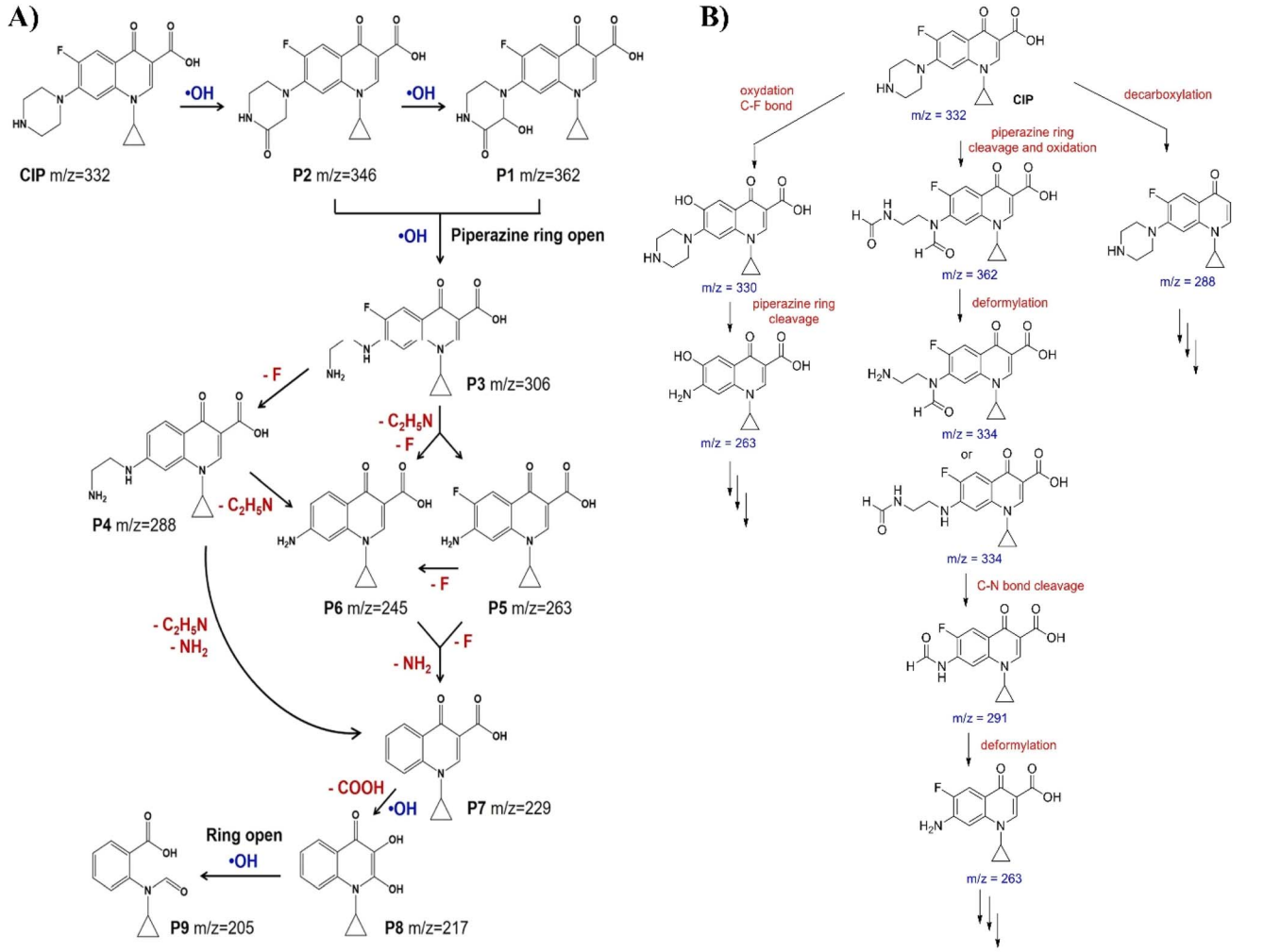

Fig. 20 Schematic illustration of degradation of CIPs by doped ZnO (A) Cu-ZnO/g-C_3N_4 reused with permission from ref. 113 Copyright 2022, Elsevier. (B) ZnO/Ag(3) photocatalyst retaken with permission from ref. 114 Copyright 2023, Elsevier.

3.5. Carbon based photocatalyst

Materials based on carbon, such as graphene, graphene oxide, reduced graphene oxide, and carbon nanotubes, have greatly enhanced photocatalytic performance. These materials have a high surface area, good electrical conductivity, and a strong adsorption capacity for organic pollutants like CIP. When used as supports or co-catalysts, carbon-based materials reduce electron–hole recombination and enable effective charge carrier separation. For instance, TiO_2-rGO composites have shown a degradation efficiency of more than 95% for CIP under both UV and visible light. Similarly, CNT-ZnO hybrids' improved recyclability and long-term photostability make them suitable for continuous water treatment applications.[160] Recent studies show that carbon-based photocatalysts effectively degrade CIP. Ciprofloxacin (CIP) degradation has been mentioned the usage of both pristine g-C_3N_4 and phosphorus-doped g-C_3N_4 (P-g-C_3N_4), accomplishing removal efficiencies of 50% and 60%, respectively. The more advantageous photocatalytic hobby turned into attributed to stepped forward era of photogenerated electrons, holes, and hydroxyl radicals, at the same time as phosphorus doping reduced the bandgap from 2.70 to 2.48 eV, thereby growing the degradation performance, Fig. 24A and B demonstrate degradation mechanism for CIPs with 2% P-g-C_3N_4 photocatalyst.[161] Further upgrades were found in nanohybrids combining g-C_3N_4 with V_2O_5 nanoparticles through easy calcination technique, attaining CIP removal as much as 97%.[162]

A novel nanohybrid composed of nitrogen-doped carbon dots (NCD) deposited on bismuth molybdate and g-C_3N_4 called Bi_2MoO_6/g-C_3N_4 proven green photocatalytic degradation of CIP underneath visible mild. This photocatalyst exhibited high activity, balance, and reusability, effective degradation, as schematically and mechanistically illustrated in Fig. 24C and D respectively.[163] Similarly, a carbon-primarily based photocatalyst, g-C_3N_4/CQD/CC, was prepared by means of embedding 0-dimensional carbon quantum dots (CQDs) into one-dimensional porous tubular g-C_3N_4 on carbon fabric (CC). This material degraded 98% of CIP within 60 min under seen-light irradiation, attributed to more advantageous light absorption.[164] Wei *et al.* Synthesized round CdS nanoparticles

Table 2 ZnO based photocatalysts for ciprofloxacin degradation concentration, efficiency and kinetic parameters

S/n	Catalyst	Dosage ($g\ L^{-1}$)	Light source	Concentration of ciprofloxacin ($mg\ L^{-1}$)	Kinetics model	Rate constant (min^{-1})	Time (min)	Efficiency (%)	Ref.
1	ZnO nanoparticles	0.2	UV light	5	Pseudo 1st order	0.0029	60	48	118
2	ZnO	0.35	300 W xenon lamp	20	Pseudo 1st order	0.042	60	95	119
3	ZnO/Au nanowire	0.0375	300 W xenon lamp	2×10^{-5} mol L^{-1}	Pseudo 1st order	0.0013	120	16	120
4	ZnO/Ag_2O	0.8	250 W UV lamp	10	Pseudo 1st order	0.043	60	31	121
5	ZnO nanotube	0.035	300 W xenon lamp	2×10^{-5} mol L^{-1}	Pseudo 1st order	0.000961	120	12	120
6	γ-Fe_2O_3@ZnO	0.5	300 W xenon lamp	10	Pseudo 1st order	0.0419	60	92	122
7	ZnO/SnS_2	0.66	200 W quartz tungsten halogen lamp	40	Pseudo 1st order	0.0571	120	100	123
8	ZnO-Ag_2O/porous g-C_3N_4	0.5	500 W tungsten lamp	20	Pseudo 1st order	0.057	48	97	124
9	ZnO	0.15	9 W low pressure mercury UV lamp	10	Pseudo 1st order	0.032	140	100	125
10	N-ZnO/CdS/GO	0.5	300 W xenon lamp	15	Pseudo 2nd order	—	60	86	126

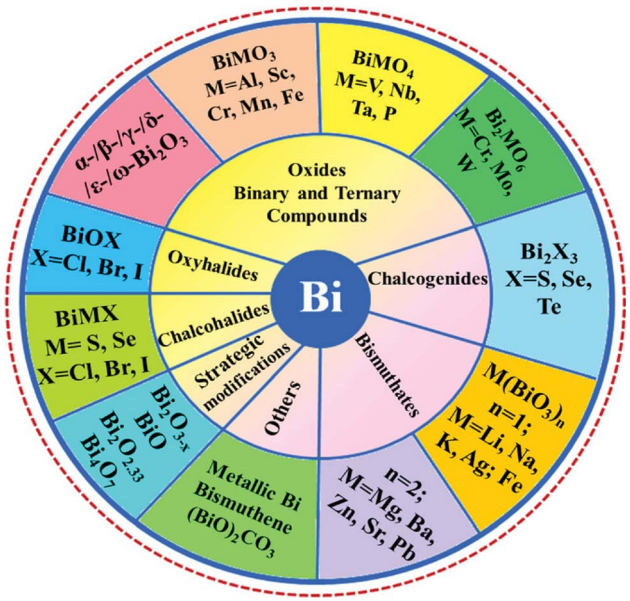

Fig. 21 Categories of bismuth (Bi) modified with permission from ref. 127 Copyright 2023, Viley-VcH.

within graphene aerogel (GA) thru a one-pot hydrothermal technique. The CdS-GA hybrids exhibited a porous shape and sturdy electric interactions, achieving CIP elimination of as much as 85.8%, demonstrating the capacity of semiconductor-GA composites for combined adsorption and photocatalytic interest.[165] Another system, CNT@MIL-115 (Fe), blended multi-walled carbon nanotubes (CNTs) with the metallic–organic framework MIL-one zero one (Fe), providing quicker charge switch and activation, ensuing in 90% CIP degradation underneath seen light. Fig. 25A depicted proposed degradation mechanism by these materials.[166] Table 5, discussing some carbon-based photocatalyst for CIPs.

3.6. Graphite

Graphitic carbon nitride (g-C_3N_4), a metal-free photocatalyst active under visible light, has gained significant attention due to its moderate bandgap (~2.7 eV).[168] Its unique layered structure and ease of synthesis from nitrogen-rich precursors make it an attractive alternative to metal oxide photocatalysts. However, pristine g-C_3N_4 suffers from challenges such as photogenerated electron–hole pair recombination and a modest surface area.[169] To enhance its photocatalytic performance, various strategies have been employed, including the formation of composites with semiconductors like TiO_2, ZnO, and $BiVO_3$, which promote charge separation and improve efficiency.[170] Porous and doped forms of g-C_3N_4 have also been studied to enhance surface reactivity. A g-C_3N_4/TiO_2 nanocomposite, demonstrated 95% CIP removal under visible light in less than 90 minutes, outperforming the component parts.[171] Fig. 25B demonstrated mechanism of CIPs photodegradation by Ag-doped-graphite-derived photocatalyst.[172]

3.7. Metal organic frameworks (MOF)

In the photocatalytic degradation of antibiotics, metal–organic frameworks (MOFs) have also been employed due to their high porosity, tunable structures, and large surface areas.[173] When used as stand-alone photocatalysts or as parts of hybrid systems, MOFs like MIL-53(Fe), UiO-66, and ZIF-8 have demonstrated encouraging outcomes. MOFs have the ability to absorb light or serve as support that improve the activity and dispersion of conventional semiconductors.[174] Under visible light, it has been demonstrated that MIL-53(Fe) and g-C_3N_4 can

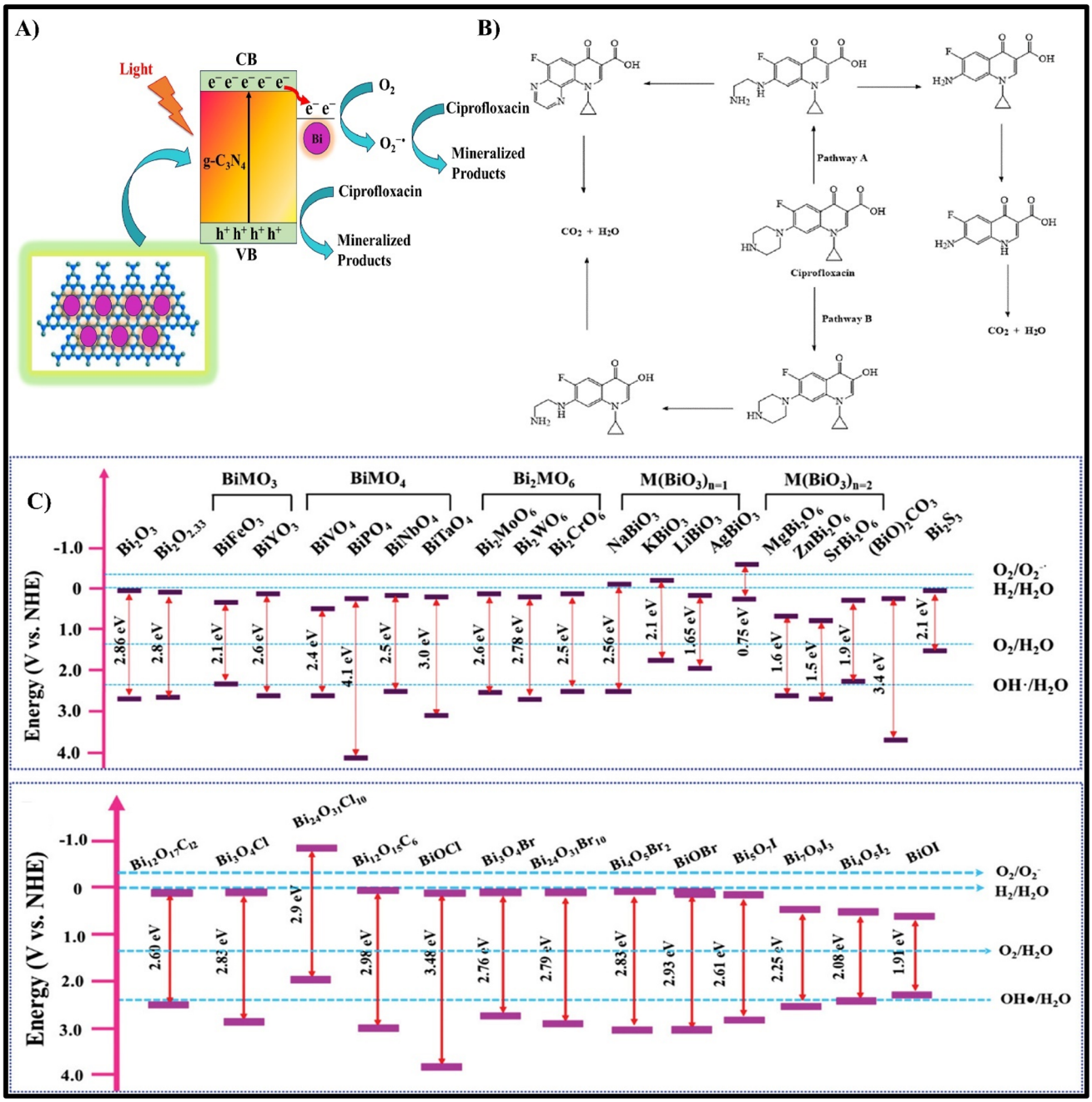

Fig. 22 (A and B) Proposed CIPs degradation mechanism followed by $BiVO_4/g\text{-}C_3N_4$ photocatalyst adopted with permission from ref. 130 Copyright 2025, Elsevier. (C) Graphical demonstration of bandgap energy of various bismuth based photocatalyst reproduced with permission from ref. 131 Copyright 2022, Elsevier.

degrade more than 90% of CIP in 90 minutes. However, MOFs' practical application is still limited by their moisture sensitivity and relatively high synthesis costs.[175]

Metal–natural frameworks (MOFs) have emerged as surprisingly versatile and efficient photocatalysts for the degradation of ciprofloxacin (CIP) due to their rather excessive surface place, tunable porosity, and bendy structural layout.[176] Composed of metal ions or clusters coordinated to natural linkers, MOFs provide abundant lively sites for pollutant adsorption and facilitate speedy mass transfer at some stage in photocatalysis.[177] Their optical and digital residences may be precisely changed through selecting suitable metal centers (along with Fe, Ti, Zr, or Co) and natural ligands, enabling sturdy absorption in the UV-seen area. Among them, Fe-primarily based MOFs (*e.g.*, MIL-100-Fe) showcase strong redox behavior and wonderful seen-mild responsiveness, whilst Zr-MOFs like UiO-66 and its derivatives provide notable aqueous balance and more advantageous ligand-to-steel charge transfer, making them appropriate platforms for photocatalytic change. Ti-MOFs such as MIL-125-(Ti) also mimic the

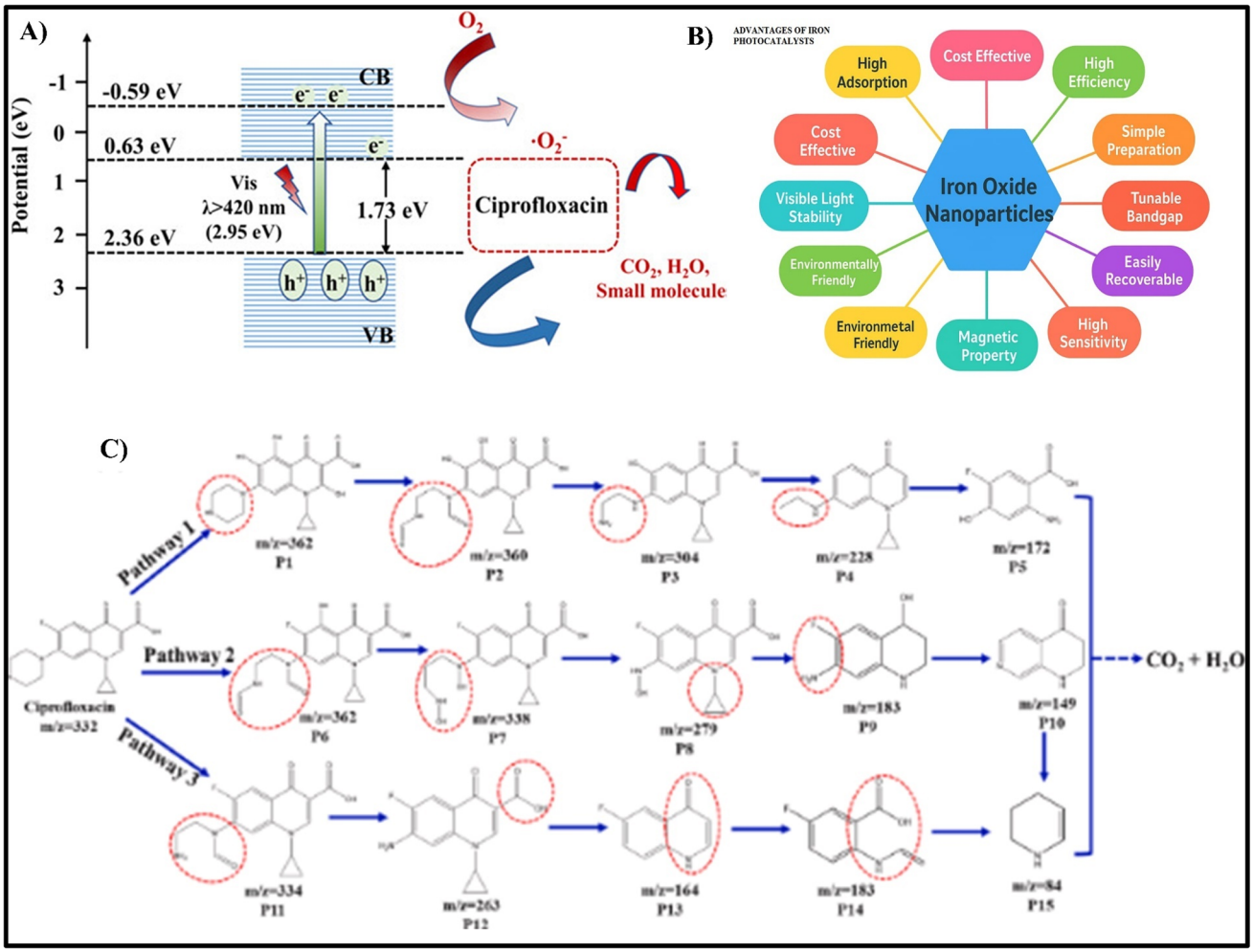

Fig. 23 (A) Scheme for BiOI-S photocatalyst for CIPs degradation reused with permission from ref. 132 Copyright 2023, Viley-VcH. (B) Advantages of Fe-photocatalyst & (C) possible degradation pathway of CIP in the A-MnO_2/Fe_2O_3@GS/H_2O_2/vis system with permission from ref. 155 Copyright 2023, Elsevier.

photoactivity of TiO_2 however with stepped forward seen-mild absorption.[178] To similarly improve their photocatalytic efficiency, numerous change techniques were implemented to MOFs, which includes steel doping, ligand functionalization, and the formation of heterojunctions with semiconductors like TiO_2, ZnO, BiOBr, or g-C_3N_4. These mixtures create green Z-scheme, S-scheme, or kind-II heterojunctions that beautify rate separation and suppress electron–hole recombination. Additionally, integrating MOFs with carbon-based totally substances inclusive of graphene oxide, decreased graphene oxide, or carbon nanotubes substantially improve conductivity, light harvesting, and structural stability. MOF-derived metallic oxide nanostructures and carbon-doped substances produced *via* controlled calcination have additionally proven outstanding photocatalytic activity towards CIP, combining the structural advantages of MOFs with the robustness of metallic oxides.[179] Fig. 25C and D depict schematic and mechanistic photodegradation of CIPs *via* MOF-derived photocatalyst called Cu_xO/MOF.[180]

During photocatalysis, MOFs generate electron–hollow pairs underneath mild irradiation, which sooner or later form reactive oxygen species (ROS) which include hydroxyl radicals ($^{\bullet}OH$), superoxide radicals ($^{\bullet}O_2^-$), and singlet oxygen ($^1O_2$). These reactive species assault the CIP molecule, initiating piperazine ring cleavage, decarboxylation, defluorination, and in the long run mineralization into CO_2 and H_2O.[181] Several MOF-based composites have demonstrated high CIP removal efficiencies, often followed pseudo-first-order kinetics and shown advanced performance compared to conventional semiconductors. Although demanding situations remain—including lengthy-term water stability, potential metal leaching, and the value of sure linkers—MOFs retain to draw large attention as promising photocatalysts for advanced water treatment packages.[182]

3.8. Photocatalytic degradation kinetics of ciprofloxacin

The efficiency and mechanism of pollutant removal under light irradiation are greatly influenced by the kinetics of photocatalytic degradation. The degradation process typically adheres to Langmuir–Hinshelwood (L–H) kinetics, which characterizes

Table 3 Bismuth based photocatalysts for ciprofloxacin degradation concentration, efficiency and kinetic parameters

S/n	Catalyst	Dosage (g L^{-1})	Light source	Concentration of ciprofloxacin (mg L^{-1})	Kinetics model	Rate constant (min^{-1})	Time (min)	Efficiency (%)	Ref.
1	BiOBr	0.5	400 W halogen lamp	5	Pseudo 1st order	0.0272	140	100	138
2	RGO/$BiVO_4$	0.2	300 W xenon lamp	10	—	—	60	68	139
3	$BiPO_4$	0.3	250 W high pressure Hg lamp	10	—	—	90	100	140
4	Er/BiOBr	0.1	300 W xenon lamp	10	—	—	360	61	141
5	BiOCl/titanium phosphate	0.4	300 W xenon lamp	5	—	—	5	100	142
6	BiOBr	0.6	300 W xenon lamp	20	Pseudo 1st order	0.0164	180	95	143
7	Bi_3TaO_7 QDs/g-C_3N_4	0.5	86 W blue LED lamp	10	Pseudo 1st order	0.198	120	91	144
8	BiOBr nanoflake/covalent triazine framework	0.2	500 W xenon lamp	10	Pseudo 1st order	0.0102	50	62	145
9	Ag modified P-doped ultrathin g-C_3N_4 nanosheets/$BiVO_4$	1	300 W xenon lamp	10	Pseudo 1st order	0.0203	120	93	146
10	Bi_2S_3/g-C_3N_4	0.625	350 W xenon lamp	20	—	—	120	65	147
11	Pt-$BiVO_4$	1.5	150 W tungsten halogen lamp	10	—	—	60	92	148
12	BiOCl half shells	1	500 W xenon lamp	10	Pseudo 1st order	0.0569	60	91	149
13	BiOCl nanosheets	1	500 W xenon lamp	10	Pseudo 1st order	0.0173	60	50	149
14	BiOBr-Bi_2MoO_6	—	300 W xenon lamp	10	—	—	120	85	144
15	Graphene-like BN/BiOBr	0.5	300 W xenon lamp	10	—	—	300	81	150

the interaction between the organic molecules and the photocatalyst surface's active sites.[183] This model states that the rate of degradation is determined by the adsorption of reactant molecules onto the catalyst and their subsequent reaction with reactive species produced by photolysis, such as superoxide anion radicals ($O_2^{\bullet -}$) and hydroxyl radicals ($^{\bullet}OH$).[184] Degradation frequently occurs at low pollutant concentrations according to pseudo-first-order kinetics, in which the rate of reaction is exactly proportional to the pollutant's initial concentration.[185] Higher concentrations, however, cause the photocatalyst surface's active sites to become saturated, deviating from first-order behavior and possibly shifting the reaction toward zero-order kinetics. The apparent rate constant is greatly influenced by variables like pH, light intensity, catalyst dosage, and the presence of electron acceptors.[186,187] In addition to offering insights into the pathways of degradation, kinetic studies aid in the optimization of operating conditions to maximize photocatalytic efficiency in environmental applications. Table 6 demonstrated various kinetic models for photocatalytic system.

3.9. Factors affecting the photocatalytic degradation efficiency of ciprofloxacin (CIP)

The efficiency of ciprofloxacin (CIP) photocatalytic degradation is strongly tormented by various operational and environmental elements. Key effects encompass the overall mineralization charge, the manufacturing of reactive oxygen species (ROS), and the interactions among the pollutant and the photocatalyst. These factors must be understood in order to optimize

Table 4 Iron-based photocatalysts for ciprofloxacin degradation concentration, efficiency and kinetic parameters

Photocatalyst	Irradiation source	Catalyst dosage	Concentration of ciprofloxacin	Time (min)	Reaction kinetics	Rate constant	Degradation efficiency (%)	References
Ni-doped α-Fe_2O_3/g-C_3N_4	Solar light	15 mg	10 mg L^{-1}	120	Pseudo-1st order	0.015 min^{-1}	82.1	156
FeS/FeO@10% 2D TiO_2-*x*	Visible light	0.1 g	20 mg L^{-1}	180	—	0.0121 min^{-1} (PPS) 0.0176 min^{-1} (H_2O_2)	90 (PPS) 100 (H_2O_2)	157
$NiFe_2O_4$@chitosin	Visible light	1.0 g L^{-1}	5 mg L^{-1}	120 120	Pseudo-1st order	0.032 min^{-1}	100	158
$FeTiO_3$/Fe-doped g-C_3N_4	Visible light	0.5 g L^{-1}	30 mg L^{-1}	120	Pseudo-1st order	0.0296 min^{-1}	93.4	159

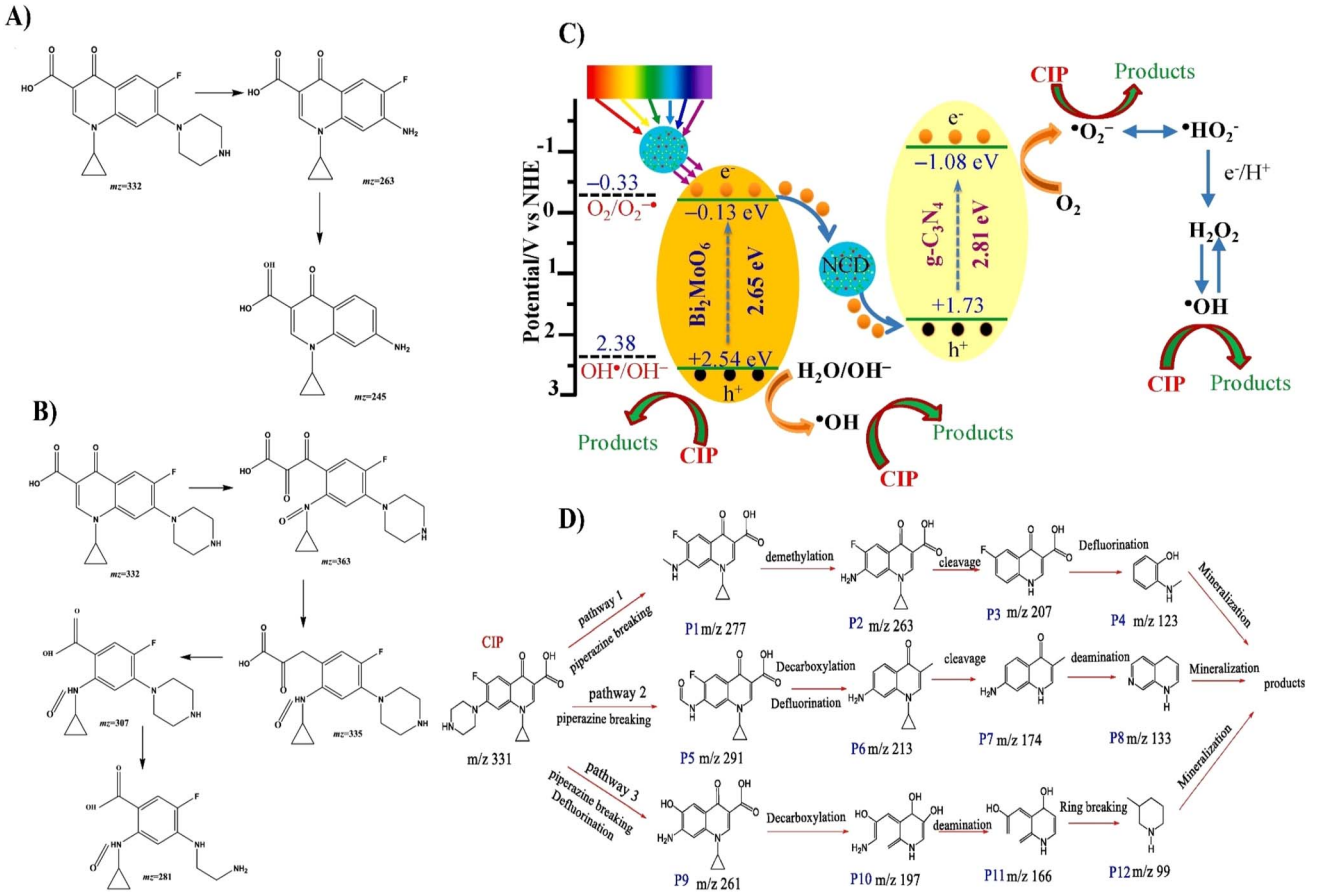

Fig. 24 (A and B) Proposed CIPs degradation mechanism by 2% P-g-C_3N_4 photocatalyst retaken with permission from ref. 161 Copyright 2024, Springer. (C and D) Z-scheme mechanism and mechanistic degradation of CIPs by NCD@BMCN under visible-light irradiation respectively reproduced with permission from ref. 163 Copyright 2021, Elsevier.

experimental conditions and scale up photocatalytic processes in real water treatment systems.[194]

3.9.1. pH and ionic strength. The pH impacts both the surface charge of the photocatalyst and the speciation of CIP in water. Due to its carboxylic and amino practical agencies, CIP can exist in distinct ionic forms relying on the pH: cationic at low pH, zwitterionic near neutral pH, and anionic at high pH, in line with its acid–base equilibria.[195] Adsorption, a requirement for effective photocatalytic degradation, is directly impacted by electrostatic interactions between these species and the photocatalyst surface. Additionally, pH affects ROS production; for example, alkaline environments produce more surface hydroxide ions, which photogenerated holes can easily oxidize to ˙OH radicals. Certain anions, such as Cl^- and HCO_3^-, can scavenge radicals, while others, such as SO_4^{2-}, can contribute to the production of secondary radicals' pH and ionic strength. Ionic strength is influenced by dissolved salts and can either promote or inhibit degradation, depending on the type of ions. The solution since pH affects the generation of radicals and the mechanism by which the contaminants are degraded, it is an important factor in the advanced oxidation process[196] The degradation fee of CIP is ruled by the blended actions of each kinds of radicals, with their relative contributions various consistent with the answer pH.[197] Additionally, chemical speciation and ionization significantly impact pollutant degradation.[198] CIP is a zwitterionic molecule, containing a charged piperazine ring and a negatively charged carboxyl institution. At pH values beneath its first pK_a (6.16), protonation takes place, that can inhibit reactions with electrophilic radicals. Conversely, while the pH exceeds its 2nd pK_a (8.23), deprotonation enhances the novel-mediated degradation of CIP.[199] This twin conduct highlights the full-size impact of protonation and deprotonation on CIP's interaction with reactive radicals. Importantly, the combined action of sulfate and hydroxyl radicals drives CIP degradation, which accounts for the highly strong rate regular throughout different pH tiers. Consequently, thermally activated persulfate-based totally AOPs can effectively degrade pollution in wastewater over a huge pH variety.[200] As a result, thermally activated PS-based AOP can break down pollutants in wastewater across a wide pH range. The overall scenario of the given description is proposed in Fig. 26A and B show pH effect on CIPs degradation.[201]

3.9.2. Initial concentration of ciprofloxacin. The initial concentration of CIP affects degradation kinetics by determining the number of molecules competing for ROS. While ROS depletion and the buildup of intermediate products at high

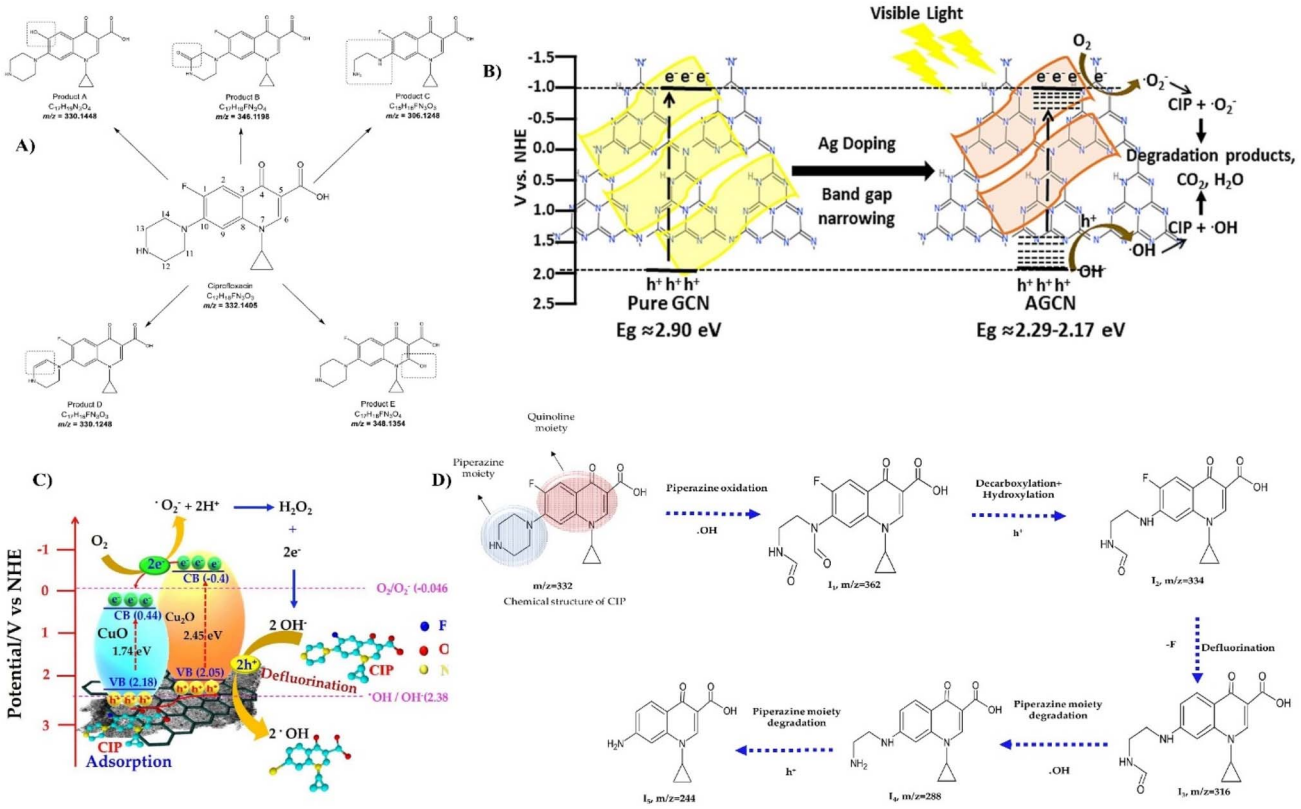

Fig. 25 (A) CNT@MIL-Fe based catalytic CIPs degradation & (B) Ag-doped-graphite derived photocatalyst adopted with permission from ref. 172 Copyright 2024, Elsevier. (C and D) Schematic and mechanistic representation of CIPs photodegradation Cu_xO/MOF reproduced with permission from ref. 180 Copyright 2023, mdpi.

concentrations may stop further degradation, abundant ROS in relation to pollutant molecules at low concentrations cause higher degradation rates.[202,203] Moreover, high concentrations of CIP may reduce the effective photon flux that reaches the photocatalyst surface by obstructing light transmission through the solution. To look at the effect of the preliminary CIPF attention at the photocatalytic overall performance of green 5% Hy-Co-ZnO NPs, a series of experiments were conducted at a catalyst dosage of 1.0 g L^{-1} and pH 7, the usage of varying CIPF starting concentrations ($C = 10$, 20, 30, 40, and 50 ppm). As the initial concentration of CIPF increases, Fig. 26C shows a clear decline in degrading efficiency. The findings suggest that at higher starting concentrations, CIPF photodegradation may be inhibited by the saturation of the Co-ZnO surface. This is because fewer photons would reach the catalyst surface at greater CIPF concentrations due to increased competition for the active sites. Consequently, fewer electron–hole pairs and hydroxyl radicals (˙OH) are produced.[204]

3.9.3. Photocatalyst dosage. The amount of photocatalyst determines the total number of active sites available to produce ROS. An increase in dosage usually improves degradation rates until a certain point, when light scattering and particle aggregation reduce effective irradiation and hinder photocatalytic efficiency.[205] Optimizing the catalyst loading is important to

Table 5 Carbon based photocatalysts for ciprofloxacin degradation concentration, efficiency and kinetic parameters

Photocatalyst	Irradiation source	Catalyst dosage	Concentration of ciprofloxacin	Time (min)	Reaction kinetics	Rate constant	Degradation efficiency (%)	Ref.
NCD@HMCN	Visible light	1.0 g L^{-1}	1.0 mg L^{-1}	30	Pseudo 1st order	0.16 min^{-1}	99.5	163
CNT@MIL-101(Fe)	Visible light	0.5 g L^{-1}	3.02	45	Pseudo 1st order	0.000685 s^{-1}	90	166
Cds-GA	Visible light	5.0 mg	20.0 mg L^{-1}	60	—	—	85.8	165
g-C_3N_4/CQD/CC	Visible light	—	5.0 mg L^{-1}	60	—	—	99	167
V_2O_5/g-C_3N_4	Visible light	0.1 g	10.0 mg L^{-1}	150	Pseudo 1st order	0.0152 min^{-1}	90.17	162

Table 6 Kinetic models of photocatalyst system

No	Phocatalyst system	Light source	Kinetic model	Rate constant (K)	Degradation efficiency	Reference
1	$Fe_{3-x}O_4$–TiO_2 + H_2O_2	UV	Pseudo-1st order	0.05 min^{-1}	~50% Reduction in ~17 min	188
2	Ti_2 (bare)	UV (16 W lamp)	Pseudo-1st order	0.0063 min^{-1}	57% (120 min)	189
3	ZnO/g-C_3N_4	Visible	Not quantified	—	~93.8% (~5× faster than g-C_3N_4)	190
4	TiO_2@g-C_3N_4@biochar (Z-scheme)	UV-visible	Not quantified	—	99.3% (UV-vis), 89.2% (VIS)	191
5	SiC/g-C_3N_4 + persulfate (SCN/PS)	Visible	Pseudo-1st order	0.132 min^{-1} (SCN/PS), 0.0102 min^{-1} (SCN only)	~95% (30 min)	192
6	TiO_2/SnO_2/g-C_3N_4 (ternary heterojunction)	Solar simulated	Not quantified	—	>97%	193

balance surface reactivity and light utilization. At high dosages, catalyst particles tend to agglomerate all through photo-degradation, which reduces the to be had floor area and diminishes the efficiency of drug elimination. Additionally, exceeding the surest catalyst amount can growth answer turbidity, limiting UV mild penetration and in addition lowering degradation overall performance. Conversely, growing the catalyst inside the best range complements the quantity of lively websites and promotes the generation of radicals that power the degradation procedure.[206] Fig. 26D, depicted the catalytic dosage effect on CIPs degradation.[207]

3.9.4. Temperature. Temperature has very little effect on photocatalytic processes because photons, not heat, are the primary driving force.[208] Nevertheless, moderate temperature increases can enhance diffusion rates and adsorption kinetics, whereas extremely high temperatures may promote the desorption of CIP and intermediates, reducing surface contact with ROSA collection of experiments were finished using green 5% Hy-Co-ZnO NPs at temperatures starting from 25 to 45 °C to research the effect of temperature on the photodegradation price of ciprofloxacin. Fig. 26E illustrates the effect on temperature on ciprofloxacin photocatalytic degradation at an initial attention of 30 ppm and a catalyst dose of 1.0 g L^{-1}. The

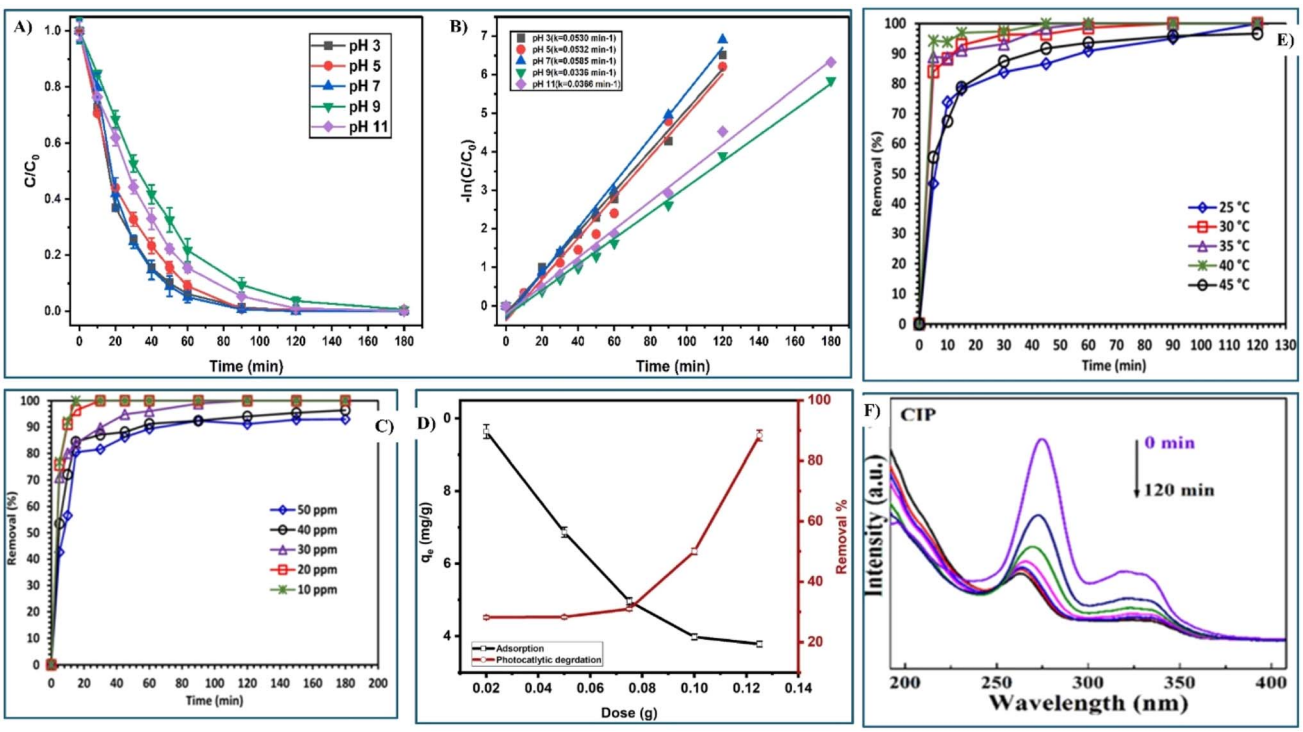

Fig. 26 Effect of various parameter on CIPs degradation. (A and B) pH effect reused with permission from ref. 201 Copyright 2025, Elsevier. (C) CIPs initial conc. Effect retaken with permission from ref. 204 Copyright 2024, nature. (D) Catalyst dosage effect adopted with permission from ref. 207 Copyright 2025, nature. (E and F) Effect of temperature and light intensity respectively reproduced with permission from ref. 204 Copyright 2024, nature.

consequences display that the degradation fee increases with temperature, as higher temperatures enhance the technology of unfastened radicals and reduce the recombination of electron–hollow pairs. As the temperature increased up to 45 °C, the kinetics of deterioration slowed. One possibility could be that heat stress increases the stability of fluoroquinolones.[204]

3.9.5. Light intensity. For efficient excitation of electrons from the valence band to the conduction band, the energy and spectral distribution of the light supply need to correspond to the bandgap of the photocatalyst. While UV mild is powerful for activating wide bandgap semiconductors like TiO_2, seen-light-responsive materials—along with doped TiO_2, g-C_3N_4, or heterojunction composites—enable the utilization of sun energy. The production of electrons and holes is accelerated by increasing light intensity, but excessive intensities can lead to recombination because they produce carriers too rapidly without providing adequate reaction time.[209] The study examined how light intensity affects photocatalytic degradation of CIP ($C_0 = 10$ mg L^{-1}, pH = 6.8). Light intensities ranging from 7.7 to 42 W m^{-2} were tested. Fig. 26F (ref. 204) shows that higher light intensity accelerates photocatalytic breakdown. As light intensity increases, photoactive species (electron–hole pairs) are generated on the semiconductor surface, leading to faster photocatalytic destruction of CIP.[210]

3.10. Comparison with other advanced oxidation processes (AOPs)

Photocatalysis has gained widespread recognition due to its affordability, sustainability, and ease of integration into water treatment systems. However, when compared to other advanced oxidation processes (AOPs), several kinetic, operational, and matrix sensitivity differences are particularly noticeable. For example, ciprofloxacin degradation is typically higher in UV-based AOPs such as UV/chlorine and UV/persulfate (UV/PS), especially in reclaimed water. These systems outperform conventional UV and UV/H_2O_2 setups due to their ability to generate potent reactive species, such as sulfate and chlorine radicals. Common water contaminants like organic matter, bicarbonates, and chlorides, however, can significantly reduce their effectiveness. Compared to UV/PMS systems (0.145 min^{-1}) and UV/sulfite systems (0.269 min^{-1}), UV/PS systems have shown pseudo-first-order rate constants of up to 0.752 min^{-1} under ideal conditions. The latter also facilitate effective defluorination at alkaline pH through hydrated electron pathways. Attention has also been drawn to the ability of catalytic sulfate radical AOPs, such as $MnFeO_4$-peroxymonosulphate (MPS/MFO) systems, to achieve high CIP removal (~92%) over a broad pH range. However, these systems have the potential to increase ionic strength and introduce secondary sulfate ions, which could limit the environmental acceptability of treated water.[211] Ozone-based processes represent yet another competitive alternative. Ozone alone can remove more than 98% of CIP, and ozone and H_2O_2 together significantly increase TOC removal (>90%) compared to ozone alone (~15%). Energy-efficient variants, such as ozone microbubble diffusion systems with aerator pumps, have shown improved degradation efficiency (83.5% *vs.* 60.9%) and energy utilization (~0.146 g kW^{-1} h^{-1}).[212] Several studies have demonstrated the high mineralization capacity of electrochemical AOPs, particularly the electro-Fenton (EF) process, which removes more than 94% of the total organic carbon (TOC). EF systems produce hydroxyl radicals *in situ* by catalyzing reactions between Fe^{2+} and electrochemically produced H_2O_2. Other electrochemical technologies like photo electrocatalysis, anodic oxidation, and combined techniques using persulfate or ultrasound often yield mineralization rates above 90%, despite the fact that these systems typically require high operating energy and maintenance.[213] An additional useful technique that commonly makes use of nano-CuO_x and H_2O_2 is catalytic wet peroxide oxidation (CWPO). At high temperatures (~95 °C), it has been demonstrated to remove CIP significantly (~86.8%) and reduce COD moderately (~54.9%). Although CWPO can effectively break down complex molecules like ciprofloxacin through processes like decarboxylation and ring hydroxylation, its use may be limited due to its need for high temperatures and metallic catalysts.[214] However, photocatalysis offers a more flexible and eco-friendlier platform, especially when using visible-light active materials like doped ZnO composites or TiO_2/g-C_3N_4 as shown in Fig. 27.[215] Although its degradation rates may be slightly lower than those of radical-based AOPs under controlled lab conditions, photocatalysis has the advantages of operating in mild conditions, using solar energy, and being compatible with catalyst immobilization strategies for easy reuse. However, issues like slower kinetics in turbid or colored water, catalyst deactivation, and occasionally limited mineralization potential continue to be challenges. Hybrid systems that combine photocatalysis with other AOPs, like photocatalysis plus persulfate or photo electrocatalysis, may offer the most promising path forward to balance efficiency, cost, and environmental sustainability.

3.11. Future prospects and research gaps

Effective photocatalysts for the degradation of ciprofloxacin (CIP) have been developed to a great extent, but several

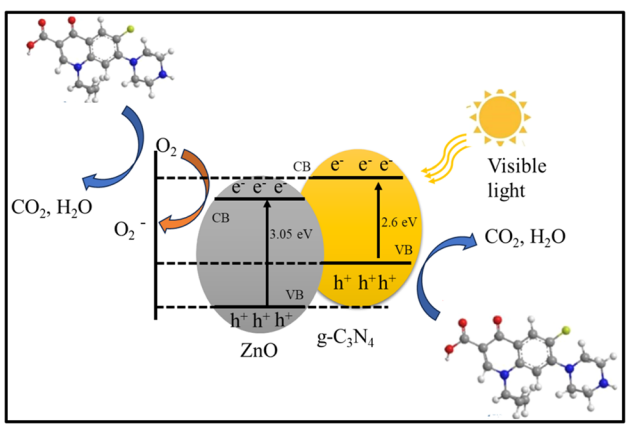

Fig. 27 Photocatalytic degradation mechanism of CIP on the TiO_2@g-C_3N_4@BC under UV-vis light irradiation reproduced with permission from ref. 215 Copyright 2025, nature.

significant problems and research gaps still limit their practical applications.[216] These limitations must be overcome to advance photocatalytic water treatment technologies from laboratory research to broad adoption. To function properly, most conventional photocatalysts, such as ZnO and TiO_2, require strong solar irradiation or artificial UV light sources. Since UV only accounts for around 5% of solar energy, the systems' overall energy efficiency and viability are severely limited.[217] For environmentally friendly treatment processes, future research must focus on developing visible-light-active photocatalysts that can effectively capture the broader solar spectrum (for example, by band gap engineering, doping, or heterojunction formation). Although many photocatalysts achieve high removal of CIP (above 90%), total mineralization, as measured by the removal of total organic carbon (TOC), is often much lower. This leads to the creation of potentially dangerous or biologically active intermediates.[218] Future studies should investigate combining photocatalysis with other procedures (like ozonation, biological treatment, or electrochemical methods) to fully detoxify and mineralize antibiotics. In slurry-based systems, catalyst separation remains a major operational challenge, especially for large-scale applications. Magnetic recovery, membrane filtration, and immobilization techniques (like coating on glass, membranes, or ceramics) have shown promise, but they usually lead to a trade-off between surface area and light exposure.[219] Future designs should prioritize scalable reactor configurations that allow for easy catalyst reuse and effective light penetration without compromising photocatalytic activity. Numerous reactor designs, including batch, packed-bed, and tubular reactors, have been studied; however, few of these studies have connected lab-scale performance to pilot or full-scale deployment.[220] Examples of parameters that are frequently disregarded in early-stage research include photon flux distribution, flow dynamics, and hydraulic retention time (HRT). To evaluate viability at the municipal or industrial scales, future research must prioritize techno-economic analyses, pilot testing under realistic water matrices, and scale-up modeling.

Real wastewater contains ions (like Cl^-, SO_4^{2-}, and HCO_3^-), natural organic matter (NOM), and other micropollutants that can either inhibit photocatalytic activity or compete with target pollutants for reactive species. The artificial or ultrapure solutions used in many published studies are not representative of the environment. Thus, photocatalyst performance in complex water matrices, including surface waters, hospital wastewater, and pharmaceutical effluents, should be systematically investigated in future research.[221] Although photocatalysis can degrade CIP, the nature and toxicity of the intermediate products are not always well understood. Sometimes, intermediates can retain their antimicrobial qualities or even become more toxic than the parent compound. Comprehensive identification of degradation products using state-of-the-art techniques (LC-MS/MS, FTIR, and NMR) in combination with bioassays or ecotoxicological evaluations is essential to confirming water safety following treatment.[222] The lack of standardized methods for assessing photocatalytic efficiency, which include variations in light intensity, reactor volume, and catalyst dosage, makes it difficult to compare results from various investigations. Additionally, many reports employ simple pseudo-first-order kinetics without accounting for mass transfer limitations, catalyst deactivation, or radical scavenging effects.[223] Future studies should focus on standardized testing conditions in addition to comprehensive kinetic and mechanistic modeling.

4. Conclusion

The increasing detection of ciprofloxacin (CIP) in aquatic environments poses a serious threat to public safety and ecological health due to its persistence, bioaccumulation potential, and role in antibiotic resistance. Photocatalytic degradation has emerged as a practical and sustainable way to remove CIP from water systems, as it generates highly reactive species when exposed to light, breaking down complex pharmaceutical molecules. Various photocatalytic materials, including metal oxides (like TiO_2 and ZnO), doped semiconductors, heterojunction composites, and magnetic nanostructures, have demonstrated effective CIP removal under UV and visible light, with multiple studies achieving degradation efficiencies above 90%. Among these, the most promising catalyst design strategies identified in this review include:

➢ Doping with metal or non-metal elements such as Fe, Ag, N, or C to modify the bandgap and enhance light absorption, allowing for visible-light activation and improving photocatalytic efficiency.

➢ Heterojunction formation, which effectively improves charge carrier separation and reduces recombination rates, thus enhancing the efficiency of photocatalytic degradation.

➢ Integration with carbon-based materials, such as graphene oxide or reduced graphene oxide (rGO), which further enhances photocatalyst performance by improving conductivity and light harvesting capabilities.

However, significant barriers to practical implementation remain, including low mineralization rates, limited visible-light response, issues with catalyst recovery, and poor scalability in real wastewater conditions. Advanced photocatalysts with enhanced light absorption, stability, and reusability must be developed alongside optimized reactor configurations to bring this technology closer to full-scale deployment. Future research must focus on performance validation in realistic environmental matrices and thorough assessment of degradation intermediates, ensuring safe and effective treatment of pharmaceutical pollutants.

Conflicts of interest

The authors declare that they have no known competing financial interests or personal relationships that could have appeared to influence the work reported in this paper.

Data availability

Since this manuscript is a review paper, no new experimental data were generated or analyzed in the course of this work. All data supporting the findings of this study are available within

the cited references, which have been duly acknowledged in the manuscript.

References

1 P. M. Dowling, Fluoroquinolones, in *Antimicrobial Therapy in Veterinary Medicine*, 2024, pp. 325–343.
2 M. Safdari, M. Mahdi Emamjomeh and A. Rezaee, Ciprofloxacin removal as an emerging contaminant using electrochemical advanced reduction process: Mechanism, degradation pathway and reaction kinetic, *J. Ind. Eng. Chem.*, 2025, **145**, 441–451.
3 M. Idrees, *et al.*, Gossypium biochar supported plasmonic nZVAg-TiO2 nanocomposite for enhanced visible-light-driven photocatalytic degradation of ciprofloxacin: synthesis, characterization, and performance evaluation, *Inorg. Chem. Commun.*, 2025, 115863.
4 L. Qalyoubi, A. Al-Othman and S. Al-Asheh, Removal of ciprofloxacin antibiotic pollutants from wastewater using nano-composite adsorptive membranes, *Environ. Res.*, 2022, **215**, 114182.
5 A. Islam, *et al.*, Advanced nanocomposite materials for efficient adsorptive remediation of pharmaceutical pollutants in aquatic systems, *J. Mol. Liq.*, 2025, 129082.
6 B. M. Al-howri, S. Ismail and M. Khajavian, comprehensive review of ciprofloxacin pollution in water: sources, environmental impacts, remediation techniques, and research challenges, *Environ. Monit. Assess.*, 2025, **197**(10), 1095.
7 J. Iqbal, *et al.*, Dual-functional Ti3C2 MXene/CuFe2O4 composite for visible light-driven degradation of ofloxacin in the presence of HSO5− and production of green H2 via photo-reforming, *Chem. Eng. J.*, 2025, 168874.
8 M. Zahid, *et al.*, Photocatalytic Degradation of Norfloxacin Using Biochar Supported nZVMn/TiO_2 Nanocomposite: Synthesis, Characterization, and Performance Evaluation, *Surf. Interfaces*, 2025, 107034.
9 Y. Zhang, *et al.*, Fabrication of bimetallic metal organic frameworks functionalized electrospun polyacrylonitrile nanofibers for efficient and selective removal of ciprofloxacin: performance and mechanism, *Sep. Purif. Technol.*, 2026, **390**, 136932.
10 N. Tian, *et al.*, Theoretical study on the homogeneous and heterogeneous oxidation reactions of Cis-3-hexenyl acetate initiated by ozone, *Chem. Phys. Lett.*, 2025, 142398.
11 P. P. Mishra, *et al.*, Architecting the Z-scheme heterojunction derived g-C3N4/Gd2O3 composite for visible-light mediated photocatalytic degradation of Ciprofloxacin and Tetracycline, *J. Ind. Eng. Chem.*, 2025.
12 R. Kousar, *et al.*, Catalytic removal of synozol blue dye from aqueous solution through green synthesized iron NPs with H2O2: with addition of ECOSAR and biological investigation, *Chem. Eng. Sci.*, 2025, 122012.
13 P. P. Mishra, *et al.*, Unfolding photo-degradation/reduction activity of heterojunction-derived g-C3N4/Sm2O3 for sustainable remediation of antibiotics and organic pollutants, *J. Rare Earths*, 2025.
14 R. Chu, *et al.*, Theoretical Simulation Degradation of Bromoxynil by Ozonation in Liquid Phase: Mechanism Pathways, Kinetics, and Ecotoxicity, *Int. J. Quantum Chem.*, 2025, **125**(7), e70041.
15 Q. Qurtulen, *et al.*, Hydrothermal Synthesis and Photocatalytic Performance of CQDs/TiO_2 Nanocomposites for CIP Removal, *Water, Air, Soil Pollut.*, 2025, **237**(3), 136.
16 M. Zahid, *et al.*, Biochar-derived photocatalysts for pharmaceutical waste removal, a sustainable approach to water purification, *Appl. Surf. Sci. Adv.*, 2025, **26**, 100721.
17 M. Delnavaz, Highly efficient photocatalytic degradation of ciprofloxacin under simulated sunlight using g-C3N4/CeO2/Fe3O4 heterogeneous composite, *Ecotoxicol. Environ. Saf.*, 2025, **295**, 118175.
18 F. Ullah, *et al.*, Synergistic degradation of toxic azo dyes using Mn-CuO@Biochar: An efficient adsorptive and photocatalytic approach for wastewater treatment, *Chem. Eng. Sci.*, 2025, **302**, 120844.
19 M. Idrees, *et al.*, Advancements in photocatalytic systems for ciprofloxacin degradation, efficiency, mechanisms, and environmental considerations, *J. Mol. Liq.*, 2025, **424**, 127115.
20 B. Nas, Behavior and removal of ciprofloxacin and sulfamethoxazole antibiotics in three different types of full-scale wastewater treatment plants: a comparative study, *Water, Air, Soil Pollut.*, 2021, **232**(4), 127.
21 F. Ullah, *et al.*, Synergistic degradation of toxic azo dyes using Mn-CuO@ Biochar: An efficient adsorptive and photocatalytic approach for wastewater treatment, *Chem. Eng. Sci.*, 2025, **302**, 120844.
22 S. W. Alberti, Adsorption of ciprofloxacin from aqueous media by activated carbon: a review, *Water Conserv. Sci. Eng.*, 2024, **9**(1), 26.
23 Z. U. H. Khan, *et al.*, Electrochemical Advanced Oxidation Processes as a feasible approach towards treatment of pesticides contaminated water and environmental sustainability: A review, *J. Water Proc. Eng.*, 2025, **70**, 107083.
24 Q. Yang, Antibiotics: an overview on the environmental occurrence, toxicity, degradation, and removal methods, *Bioengineered*, 2021, **12**(1), 7376–7416.
25 H. Liu, The application of UV/O3 process on ciprofloxacin wastewater containing high salinity: performance and its degradation mechanism, *Chemosphere*, 2021, **276**, 130220.
26 M. Arshad, *et al.*, Synergistic design of an NiCo@ BC–MOF derivative for enhanced energy storage and photocatalytic applications, *RSC Adv.*, 2025, **15**(59), 50666–50681.
27 S. K. Ramachandran and P. Sathishkumar, Membrane-based techniques for pollutants removal: an outlook on recent advancements, *Curr. Opin. Environ. Sci. Health*, 2023, **36**, 100513.
28 M. Aftab, *et al.*, Synergistic effects of H 2 O 2 on the performance of nano-zero-valent manganese biochar (nZVMn/PBC) for the treatment of chlorpyrifos from aqueous solution, *RSC Adv.*, 2025, **15**(52), 44229–44245.

29 S. Shurbaji, P. T. Huong and T. M. Altahtamouni, Review on the visible light photocatalysis for the decomposition of ciprofloxacin, norfloxacin, tetracyclines, and sulfonamides antibiotics in wastewater, *Catalysts*, 2021, **11**(4), 437.
30 M. Aftab, *et al.*, Advanced oxidation processes for pesticide degradation: a comprehensive review on the role of nano zero-valent metals and persulfate activation, *RSC Adv.*, 2025, **15**(48), 40619–40654.
31 G. Zhang, *et al.*, Endogenous iron-enriched biochar loaded nickel-foam cathode in electro-Fenton for ciprofloxacin degradation: performance, mechanism and DFT calculation, *Chem. Eng. J.*, 2024, **498**, 155446.
32 X. Zhang, *et al.*, Cellulosic composite adsorbent prepared via high-speed shear induced regeneration and chemical modification for ciprofloxacin removal, *Sep. Purif. Technol.*, 2025, **362**, 131854.
33 Y. Jia, *et al.*, Ciprofloxacin degradation in anaerobic sulfate-reducing bacteria (SRB) sludge system: Mechanism and pathways, *Water Res.*, 2018, **136**, 64–74.
34 Y. Xu, *et al.*, Unravelling ciprofloxacin removal in a nitrifying moving bed biofilm reactor: Biodegradation mechanisms and pathways, *Chemosphere*, 2023, **320**, 138099.
35 E. Boahen, L. Owusu and S. O. Adjei-Anim, A comprehensive review of emerging environmental contaminants of global concern, *Discover Environ.*, 2025, **3**(1), 144.
36 K. Anbarasu and D. Yuvarajan, Pharmaceutical Pollution in Soil and Water and Its Impacts On Human Health and the Environment, *Water Air Soil Pollut.*, 2025, **236**(13), 877.
37 M. S. Javed, Advanced materials for photocatalytic removal of antibiotics from wastewater, *J. Alloys Compd.*, 2025, **1010**, 177926.
38 H. Taha, A. Zaher and N. Shehata, Optimization and kinetic modeling of ciprofloxacin adsorption and photocatalytic degradation in water, *Sci. Rep.*, 2025, 43370.
39 M. A. Abdel-Gawad, Synthesis, Characterization, DNA Binding, Biological Evaluation, and Molecular Docking Approaches of Ternary Copper (II) Complexes Involving Ciprofloxacin With Glycine and Phenylalanine, *Chem. Biodiversity*, 2025, e00481.
40 K. Lazarova, Removal of Ciprofloxacin from Aqueous Solutions by Waste-Pretreated Ganoderma resinaceum Biomass: Effect of Process Parameters and Kinetic and Equilibrium Studies, *Processes*, 2025, **13**(12), 3920.
41 D. Seibert, Application of cork as adsorbent for water and wastewater treatment using ciprofloxacin as pharmaceutical model, *Int. J. Environ. Sci. Technol.*, 2025, **22**(5), 3021–3038.
42 B. M. Al-Howri, Comprehensive review of ciprofloxacin pollution in water: sources, environmental impacts, remediation techniques, and research challenges, *Environ. Monit. Assess.*, 2025, **197**(10), 1–47.
43 D. M. Campoli-Richards, *et al.*, Ciprofloxacin: a review of its antibacterial activity, pharmacokinetic properties and therapeutic use, *Drugs*, 1988, **35**(4), 373–447.
44 M. Sarafraz, *et al.*, A global systematic, review-meta analysis and ecological risk assessment of ciprofloxacin in river water, *Int. J. Environ. Anal. Chem.*, 2022, **102**(17), 5106–5121.
45 B. M. Al-Howri, S. Ismail and M. Khajavian, comprehensive review of ciprofloxacin pollution in water: sources, environmental impacts, remediation techniques, and research challenges, *Environ. Monit. Assess.*, 2025, **197**(10), 1–47.
46 M. Aftab, Advanced oxidation processes for pesticide degradation: a comprehensive review on the role of nano zero-valent metals and persulfate activation, *RSC Adv.*, 2025, **15**(48), 40619–40654.
47 J. A. Silva, Advanced Oxidation Process in the Sustainable Treatment of Refractory Wastewater: A Systematic Literature Review, *Sustainability*, 2025, **17**(8), 3439.
48 M. Ferre, Advanced Oxidation Processes and Adsorption Technologies for the Removal of Organic Azo Compounds: UV, H2O2 and GAC, *Water*, 2025, **17**(2), 212.
49 M. H. Hemaily Abd Elmawgood, Application of direct and indirect oxidation techniques for degradation of some colored organic pollutants in aqueous solution, *J. Basic Environ. Sci.*, 2025, **12**(3), 152–181.
50 S. Sun, *et al.*, Identification and Mechanistic Analysis of Toxic Degradation Products in the Advanced Oxidation Pathways of Fluoroquinolone Antibiotics, *Toxics*, 2024, **12**, 203, DOI: 10.3390/toxics12030203.
51 M. Safdari, Ciprofloxacin removal as an emerging contaminant using electrochemical advanced reduction process: mechanism, degradation pathway and reaction kinetic.Journal of, *Ind. Eng. Chem.*, 2025, **145**, 441–451.
52 Y. Wang, Carbonaceous materials in structural dimensions for advanced oxidation processes, *Chem. Soc. Rev.*, 2025, **54**, 2436–2482.
53 P. V. Nidheesh, Generation, properties, and applications of singlet oxygen for wastewater treatment: a review, *Environ. Chem. Lett.*, 2025, **23**(1), 195–240.
54 S. Kaur, K. Kaur, and S. Maheshwari, Efficiency comparison of hybrid advanced oxidation processes for removal of ciprofloxacin from water, in *Advanced Oxidation Process-Based Integrated and Hybrid Technologies for Degradation of Pharmaceuticals and Personal Care Products*, Elsevier, 2025, pp. 365–376.
55 M. Aftab, Synergistic effects of H2O2 on the performance of nano-zero-valent manganese biochar (nZVMn/PBC) for the treatment of chlorpyrifos from aqueous solution, *RSC Adv.*, 2025, **15**, 44229–44245.
56 H. Milh, Degradation of ciprofloxacin using UV-based advanced removal processes: comparison of persulfate-based advanced oxidation and sulfite-based advanced reduction processes, *Sci. Total Environ.*, 2021, **764**, 144510.
57 F. Mu, *et al.*, Peroxymonosulfate-assisted layered MXene/flower-like C-doped SnS2 Schottky junction photocatalyst for ciprofloxacin effective degradation, *J. Alloys Compd.*, 2025, **1039**, 183354.
58 N. Akhtar, *et al.*, Visible light active CdS/CuO nanocomposites for photocatalytic degradation of

ciprofloxacin, H2 production and antimicrobial activity, *Chem. Eng. J.*, 2025, **507**, 160336.
59 S. Sambyal, *et al.*, Nanocellulose supported ZnWO4/SrTiO3/MoO3 heterojunction: Highly efficient visible light photocatalyst for ciprofloxacin degradation, *Chem. Eng. J.*, 2025, **516**, 164167.
60 P. Pascariu, C. Gherasim and A. Airinei, Metal Oxide Nanostructures (MONs) as Photocatalysts for Ciprofloxacin Degradation, *Int. J. Mol. Sci.*, 2023, **24**, 9564, DOI: 10.3390/ijms24119564.
61 M. H. Mujahid, *et al.*, Metallic and metal oxide-derived nanohybrid as a tool for biomedical applications, *Biomed. Pharmacother.*, 2022, **155**, 113791.
62 M. M. Rahman, *et al.*, Dysprosium chromite nanoparticles: A promising photocatalyst for the remediation of ciprofloxacin and methylene blue from wastewater, *J. Alloys Compd.*, 2025, **1010**, 177295.
63 P. Chen, *et al.*, Efficient removal of ciprofloxacin from water by BiOX/GaMOF S-scheme heterojunction: A synergistic effect of adsorption and photocatalysis, *Chem. Eng. J.*, 2025, **506**, 159689.
64 S.-M. Niu, *et al.*, Enhancement of photocatalytic degradation of ciprofloxacin via constructing conductive matrix, *Appl. Surf. Sci.*, 2025, **679**, 161259.
65 R. K. Paul and M. Ahmaruzzaman, Advanced photocatalytic degradation of POPs and other contaminants: a comprehensive review on nanocomposites and heterojunctions, *RSC Adv.*, 2025, **15**(38), 31313–31359.
66 M. Antonopoulou, Homogeneous and heterogeneous photocatalysis for the treatment of pharmaceutical industry wastewaters: A review, *Toxics*, 2022, **10**(9), 539.
67 K. P. Makhado, *et al.*, Current updates on p-type nickel oxide (NiO) based photocatalysts towards decontamination of organic pollutants from wastewater, *Mater. Today Sustain.*, 2024, **25**, 100664.
68 M. Surana, *et al.*, An insight decipher on photocatalytic degradation of microplastics: Mechanism, limitations, and future outlook, *Environ. Res.*, 2024, **247**, 118268.
69 N. R. Reddy, Versatile TiO2 bandgap modification with metal, non-metal, noble metal, carbon material, and semiconductor for the photoelectrochemical water splitting and photocatalytic dye degradation performance, *J. Alloys Compd.*, 2023, **935**, 167713.
70 Y. Lu, Y. Wang and J. Zhang, Semiconductor heterojunction photocatalysts with near-infrared light antennas: a review, *J. Phys. D: Appl. Phys.*, 2021, **54**(31), 313002.
71 S. Shurbaji, P. T. Huong and T. M. Altahtamouni, Review on the Visible Light Photocatalysis for the Decomposition of Ciprofloxacin, Norfloxacin, Tetracyclines, and Sulfonamides Antibiotics in Wastewater, *Catalysts*, 2021, **11**, 437, DOI: 10.3390/catal11040437.
72 R. Ghamarpoor, A. Fallah and M. Jamshidi, A Review of Synthesis Methods, Modifications, and Mechanisms of ZnO/TiO2-Based Photocatalysts for Photodegradation of Contaminants, *ACS Omega*, 2024, **9**(24), 25457–25492.
73 C. Zhu and X. Wang, Nanomaterial ZnO Synthesis and Its Photocatalytic Applications: A Review, *Nanomaterials*, 2025, **15**, 682, DOI: 10.3390/nano15090682.
74 H. AlMohamadi, *et al.*, Photocatalytic Activity of Metal- and Non-Metal-Anchored ZnO and TiO2 Nanocatalysts for Advanced Photocatalysis: Comparative Study, *Catalysts*, 2024, **14**, 420, DOI: 10.3390/catal14070420.
75 O. F. Aldosari, Photocatalytic water-splitting for hydrogen production using TiO2-based catalysts: Advances, current challenges, and future perspectives, *Catal. Rev.*, 2025, 1–38.
76 S. Sood, *et al.*, Enhancing Optoelectronic Performance Through Rare-Earth-Doped ZnO: Insights and Applications, *Photonics*, 2025, **12**, 454, DOI: 10.3390/photonics12050454.
77 A. Shahzadi, *et al.*, Advances in p- and d-block nanocatalysts for efficient photocatalytic degradation of reactive blue dye: an environmental perspective, *Environ. Technol. Rev.*, 2025, **14**(1), 517–539.
78 D. Kanakaraju, *et al.*, Pioneering TiO2/G-C3N4 Heterostructures for Enhanced Organic Pollutant Removal, *ChemistrySelect*, 2025, **10**(15), e202405101.
79 D. Jalandhara, *et al.*, $BiFeO_3$ as a Next-Generation Photocatalyst: Bridging Material Design with Environmental Remediation, *ChemPhysChem*, 2025, **26**(10), e202401092.
80 K. H. Badagoppam Haroon and S. K. Bhunia, Fenton-like Catalysts Based on Graphitic Carbon Nitride Nanosheets Decorated with Fe3O4 Nanoparticles for Removal of Colorless Tetracycline, *ACS Appl. Nano Mater.*, 2024, **7**(23), 26356–26368.
81 T. Kong, Recent advances and mechanism of plasmonic metal–semiconductor photocatalysis, *RSC Adv.*, 2024, **14**, 17041–17050.
82 N. E. Fard, *et al.*, A review on development and modification strategies of MOFs Z-scheme heterojunction for photocatalytic wastewater treatment, water splitting, and DFT calculations, *Heliyon*, 2024, **10**(13), e32861.
83 Q. Guo, *et al.*, Fundamentals of TiO2 photocatalysis: concepts, mechanisms, and challenges, *Adv. Mater.*, 2019, **31**(50), 1901997.
84 R. Krakowiak, *et al.*, Titanium Dioxide-Based Photocatalysts for Degradation of Emerging Contaminants including Pharmaceutical Pollutants, *Appl. Sci.*, 2021, **11**, 8674, DOI: 10.3390/app11188674.
85 A. Kutuzova, T. Dontsova and W. Kwapinski, Application of TiO2-Based Photocatalysts to Antibiotics Degradation: Cases of Sulfamethoxazole, Trimethoprim and Ciprofloxacin, *Catalysts*, 2021, **11**, 728, DOI: 10.3390/catal11060728.
86 S. Khan, *et al.*, Photocatalytic Dye Degradation from Textile Wastewater: A Review, *ACS Omega*, 2024, **9**(20), 21751–21767.
87 S. Danfá, *et al.*, Supported TiO2 in Ceramic Materials for the Photocatalytic Degradation of Contaminants of Emerging Concern in Liquid Effluents: A Review, *Molecules*, 2021, **26**, 5363, DOI: 10.3390/molecules26175363.

88 H. N. Dharma, *et al.*, A Review of Titanium Dioxide (TiO2)-Based Photocatalyst for Oilfield-Produced Water Treatment, *Membranes*, 2022, **12**, 345, DOI: 10.3390/membranes12030345.
89 S. Li, *et al.*, Ta3N5/CdS core–shell S-scheme heterojunction nanofibers for efficient photocatalytic removal of antibiotic tetracycline and Cr (VI): performance and mechanism insights, *Adv. Fiber Mater.*, 2023, **5**(3), 994–1007.
90 I. Idrees, *et al.*, Hybrid biochar-graphitic carbon nitride (g-C3N4) composite photocatalyst: a facile strategy for enhanced degradation of Ciprofloxacin (CIP), *Mater. Res. Express*, 2025, **12**(3), 035503.
91 Y. Wang, *et al.*, Enhanced LED light-driven antibacterial system with efficient charge transfer coordinated by Bi2WO6/TiO2 Z-scheme heterojunction, *Ceram. Int.*, 2024, **50**(6), 9307–9322.
92 T. T. Buu, *et al.*, Construction of Z-scheme heterojunction TiO2-ZnO@ Oxygen-doped gC3N4 composite for enhancing H2O2 photoproduction and removal of pharmaceutical pollutants under visible light, *Surf. Interfaces*, 2023, **43**, 103516.
93 B. Zhang, *et al.*, Degradation of tetracycline hydrochloride by ultrafine TiO2 nanoparticles modified g-C3N4 heterojunction photocatalyst: Influencing factors, products and mechanism insight, *Chin. Chem. Lett.*, 2022, **33**(3), 1337–1342.
94 M. Cai, *et al.*, Floatable S-scheme Bi2WO6/C3N4/carbon fiber cloth composite photocatalyst for efficient water decontamination, *Chin. J. Catal.*, 2023, **52**, 239–251.
95 M. Chen, *et al.*, Rational Synthesis of Spongy Fe3N@N-Doped Carbon Nanorods with Controlled Topography and Porosity for Enhanced Energy Storage Anodes in Lithium-Ion Batteries, *Langmuir*, 2024, **40**(45), 24017–24028.
96 S. N. H. Jaafar, *et al.*, Natural dyes as TIO2 sensitizers with membranes for photoelectrochemical water splitting: An overview, *Renew. Sustain. Energy Rev.*, 2017, **78**, 698–709.
97 R. Noroozi, *et al.*, Fabrication of new composite NCuTiO2/CQD for photocatalytic degradation of ciprofloxacin and pharmaceutical wastewater treatment: degradation pathway, toxicity assessment, *Sci. Rep.*, 2023, **13**(1), 16287.
98 A. Hassani, *et al.*, Heterogeneous photocatalytic ozonation of ciprofloxacin using synthesized titanium dioxide nanoparticles on a montmorillonite support: parametric studies, mechanistic analysis and intermediates identification, *RSC Adv.*, 2016, **6**(90), 87569–87583.
99 X. Van Doorslaer, *et al.*, UV-A and UV-C induced photolytic and photocatalytic degradation of aqueous ciprofloxacin and moxifloxacin: reaction kinetics and role of adsorption, *Appl. Catal., B*, 2011, **101**(3–4), 540–547.
100 F. Hassani, P. M. Nekoovaght and N. Gharib, The influence of microwave irradiation on rocks for microwave-assisted underground excavation, *J. Rock Mech. Geotech. Eng.*, 2016, **8**(1), 1–15.
101 L. Lamboni, *et al.*, Silk sericin: A versatile material for tissue engineering and drug delivery, *Biotechnol. Adv.*, 2015, **33**(8), 1855–1867.
102 T. A. Gad-Allah, M. E. Ali and M. I. Badawy, Photocatalytic oxidation of ciprofloxacin under simulated sunlight, *J. Hazard. Mater.*, 2011, **186**(1), 751–755.
103 A. Salma, *et al.*, Dependence of transformation product formation on pH during photolytic and photocatalytic degradation of ciprofloxacin, *J. Hazard. Mater.*, 2016, **313**, 49–59.
104 M. A. Abdelkareem, *et al.*, Recent progress in the use of renewable energy sources to power water desalination plants, *Desalination*, 2018, **435**, 97–113.
105 V. Chernyak, *et al.*, Liver imaging reporting and data system (LI-RADS) version 2018: imaging of hepatocellular carcinoma in at-risk patients, *Radiology*, 2018, **289**(3), 816–830.
106 S. A. Shetty, *et al.*, Intestinal microbiome landscaping: insight in community assemblage and implications for microbial modulation strategies, *FEMS Microbiol. Rev.*, 2017, **41**(2), 182–199.
107 R. K. Das, J. P. Kar and S. Mohapatra, Enhanced photodegradation of organic pollutants by carbon quantum dot (CQD) deposited Fe3O4@ mTiO2 nano-pom-pom balls, *Ind. Eng. Chem. Res.*, 2016, **55**(20), 5902–5910.
108 N. R. Faria, *et al.*, Zika virus in the Americas: early epidemiological and genetic findings, *Science*, 2016, **352**(6283), 345–349.
109 Y. Sun, *et al.*, Preparations and applications of zinc oxide based photocatalytic materials, *Adv. Sens. Energy Mater.*, 2023, **2**(3), 100069.
110 A. L. T. Zheng, *et al.*, Recent progress in visible light-doped ZnO photocatalyst for pollution control, *Int. J. Environ. Sci. Technol.*, 2023, **20**(5), 5753–5772.
111 K. Mohamed, *et al.*, Recent advances in ZnO-based nanostructures for the photocatalytic degradation of hazardous, non-biodegradable medicines, *Crystals*, 2023, **13**(2), 329.
112 F. H. Abdullah, N. H. H. A. Bakar and M. A. Bakar, Current advancements on the fabrication, modification, and industrial application of zinc oxide as photocatalyst in the removal of organic and inorganic contaminants in aquatic systems, *J. Hazard. Mater.*, 2022, **424**, 127416.
113 J.-H. Shen, *et al.*, Mechanistic insights into hydroxyl radical formation of Cu-doped ZnO/g-C3N4 composite photocatalysis for enhanced degradation of ciprofloxacin under visible light: Efficiency, kinetics, products identification and toxicity evaluation, *J. Environ. Chem. Eng.*, 2022, **10**(2), 107352.
114 M. I. Mahrsi, *et al.*, Novel ZnO/Ag nanohybrids prepared from Ag+-doped layered zinc hydroxides as highly active photocatalysts for the degradation of dyes and Ciprofloxacin, *Colloids Surf., A*, 2023, **671**, 131643.
115 A. I. Meky, *et al.*, Hydrothermal fabrication, characterization and RSM optimization of cobalt-doped zinc oxide nanoparticles for antibiotic photodegradation under visible light, *Sci. Rep.*, 2024, **14**(1), 2016.
116 I. Mukherjee, V. Cilamkoti and R. K. Dutta, Sunlight-driven photocatalytic degradation of ciprofloxacin by carbon dots

embedded in ZnO nanostructures, *ACS Appl. Nano Mater.*, 2021, **4**(8), 7686–7697.
117 H. Ye, *et al.*, CaFe2O4/Ag/ZnO z-scheme heterojunction material for photocatalytic decomposition of ciprofloxacin, *Chem. Phys. Lett.*, 2024, **842**, 141227.
118 M. El-Kemary, H. El-Shamy and I. El-Mehasseb, Photocatalytic degradation of ciprofloxacin drug in water using ZnO nanoparticles, *J. Lumin.*, 2010, **130**(12), 2327–2331.
119 F. Nekouei and S. Nekouei, Comparative study of photocatalytic activities of Zn5 (OH) 8Cl2· H2O and ZnO nanostructures in ciprofloxacin degradation: Response surface methodology and kinetic studies, *Sci. Total Environ.*, 2017, **601**, 508–517.
120 C. Bojer, *et al.*, Clinical wastewater treatment: Photochemical removal of an anionic antibiotic (ciprofloxacin) by mesostructured high aspect ratio ZnO nanotubes, *Appl. Catal., B*, 2017, **204**, 561–565.
121 Z. Zhao, D. Dua, and S. Singh, Generating natural adversarial examples, *arXiv*, 2017, preprint, arXiv:1710.11342, DOI: 10.48550/arXiv.1710.11342.
122 Y. Li, *et al.*, Demystifying neural style transfer, *arXiv*, 2017, preprint arXiv:1701.01036, DOI: 10.48550/arXiv.1701.01036.
123 S. Makama, *et al.*, A novel method for the quantification, characterisation and speciation of silver nanoparticles in earthworms exposed in soil, *Environ. Chem.*, 2015, **12**(6), 643–651.
124 J. Rong, *et al.*, Radial lens distortion correction using convolutional neural networks trained with synthesized images, in *Asian Conference on Computer Vision*, Springer, 2016.
125 M. Eskandari, N. Goudarzi and S. G. Moussavi, Application of low-voltage UVC light and synthetic ZnO nanoparticles to photocatalytic degradation of ciprofloxacin in aqueous sample solutions, *Water Environ. J.*, 2018, **32**(1), 58–66.
126 B. Huo, *et al.*, The impact of human capital on supply chain integration and competitive performance, *Int. J. Prod. Econ.*, 2016, **178**, 132–143.
127 S. Adhikari, S. Mandal and D.-H. Kim, Recent Development Strategies for Bismuth-Driven Materials in Sustainable Energy Systems and Environmental Restoration, *Small*, 2023, **19**(10), 2206003.
128 L. Chen, Review on the preparation and performance improvement methods of bismuth photocatalyst materials, *Catal. Sci. Technol.*, 202313, 5478–5529.
129 L. Zhang, *et al.*, Recent advances on Bismuth-based Photocatalysts: Strategies and mechanisms, *Chem. Eng. J.*, 2021, **419**, 129484.
130 P. Saini, *et al.*, Bismuth doped g-C3N4 composites for enhanced photocatalytic degradation of ciprofloxacin, *J. Mol. Struct.*, 2025, **1321**, 140013.
131 V. Subhiksha, S. Kokilavani and S. Sudheer Khan, Recent advances in degradation of organic pollutant in aqueous solutions using bismuth based photocatalysts: A review, *Chemosphere*, 2022, **290**, 133228.
132 N. T. T. Hai, *et al.*, Improvement of photocatalytic degradation and adsorption of ciprofloxacin by bismuth oxyiodide, *Chem. Eng. Technol.*, 2023, **46**(11), 2404–2411.
133 X. Tang, *et al.*, The fabrication of a biomass carbon quantum dot-Bi 2 WO 6 hybrid photocatalyst with high performance for antibiotic degradation, *New J. Chem.*, 2019, **43**(47), 18860–18867.
134 A. Kumar, *et al.*, DFT and experimental studies of the facet-dependent oxygen vacancies modulated WS2/BiOCl-OV S-scheme structure for enhanced photocatalytic removal of ciprofloxacin from wastewater, *Environ. Res.*, 2024, **250**, 118519.
135 W.-S. Chen, M.-H. Wu and J.-Y. Wu, Effects of Tb-doped BiVO4 on degradation of methylene blue, *Sustainability*, 2023, **15**(8), 6994.
136 X. Zeng, *et al.*, Efficient photocatalytic degradation of ciprofloxacin by doped Bi4O5I2 with Gd3+ as an electron trap: Gd3+ substitutes Bi3+ in the lattice, *J. Phys. Chem. Solids*, 2024, **188**, 111891.
137 H. Lu, *et al.*, Facile fabrication of CeO2/L-Bi2O2CO3 composite photocatalyst for removal of ciprofloxacin under visible light irradiation, *Adv. Powder Technol.*, 2024, **35**(5), 104458.
138 S. Li, *et al.*, The role of oxidative stress and antioxidants in liver diseases, *Int. J. Mol. Sci.*, 2015, **16**(11), 26087–26124.
139 C.-G. Yan, *et al.*, Standardizing the intrinsic brain: towards robust measurement of inter-individual variation in 1000 functional connectomes, *Neuroimage*, 2013, **80**, 246–262.
140 S.-L. Chen, *et al.*, Conservation and sustainable use of medicinal plants: problems, progress, and prospects, *Chin. Med.*, 2016, **11**(1), 37.
141 B. Y. Xia, *et al.*, A metal–organic framework-derived bifunctional oxygen electrocatalyst, *Nat. Energy*, 2016, **1**(1), 1–8.
142 H. Ao, *et al.*, Late Miocene–Pliocene Asian monsoon intensification linked to Antarctic ice-sheet growth, *Earth Planet. Sci. Lett.*, 2016, **444**, 75–87.
143 N. Zeng, *et al.*, Effects of physical activity on motor skills and cognitive development in early childhood: a systematic review, *BioMed Res. Int.*, 2017, **2017**(1), 2760716.
144 J. Wang, *et al.*, WebGestalt 2017: a more comprehensive, powerful, flexible and interactive gene set enrichment analysis toolkit, *Nucleic Acids Res.*, 2017, **45**(W1), W130–W137.
145 P. Isola, *et al.*, Image-to-image translation with conditional adversarial networks, in *Proceedings of the IEEE Conference on Computer Vision and Pattern Recognition*, 2017.
146 L. Deng, *et al.*, UAV-based multispectral remote sensing for precision agriculture: A comparison between different cameras, *ISPRS J. Photogrammetry Remote Sens.*, 2018, **146**, 124–136.
147 R. A. Agha, *et al.*, The SCARE 2018 statement: updating consensus Surgical CAse REport (SCARE) guidelines, *Int. J. Surg.*, 2018, **60**, 132–136.
148 C. W. Brennan, *et al.*, The somatic genomic landscape of glioblastoma, *Cell*, 2013, **155**(2), 462–477.

149 H. Mao, *et al.*, Resource management with deep reinforcement learning, in *Proceedings of the 15th ACM Workshop on Hot Topics in Networks*, 2016.
150 E. Di Angelantonio, *et al.*, Body-mass index and all-cause mortality: individual-participant-data meta-analysis of 239 prospective studies in four continents, *Lancet*, 2016, **388**(10046), 776–786.
151 M. Mishra and D.-M. Chun, α-Fe2O3 as a photocatalytic material: A review, *Appl. Catal., A*, 2015, **498**, 126–141.
152 A. Agbogu, M. Orji and A. Ekwealor, Effects of temperature on the optical properties of iron oxide (Fe2O3) thin films synthesized by chemical bath deposition, *Optik*, 2016, **127**(20), 9865–9870.
153 Y. Zhang, *et al.*, Heterogeneous degradation of organic contaminants in the photo-Fenton reaction employing pure cubic β-Fe2O3, *Appl. Catal., B*, 2019, **245**, 410–419.
154 S. D. Roy, K. C. Das and S. S. Dhar, Conventional to green synthesis of magnetic iron oxide nanoparticles; its application as catalyst, photocatalyst and toxicity: A short review, *Inorg. Chem. Commun.*, 2021, **134**, 109050.
155 X. Cai, *et al.*, Valorization of manganese residue to construct amorphous MnO2/α-Fe2O3@ geopolymer Z-scheme heterojunction for efficient Cr (VI) reduction and ciprofloxacin degradation, *J. Clean. Prod.*, 2023, **398**, 136634.
156 C. N. Lakshmi, *et al.*, Magnetically recoverable Ni-doped iron oxide/graphitic carbon nitride nanocomposites for the improved photocatalytic degradation of ciprofloxacin: Investigation of degradation pathways, *Environ. Res.*, 2024, **242**, 117812.
157 M. M. Mohamed, E. E. Abdelmonem and G. El-Sayed, Bifunctional Fe active sites on carbon nitride and titanium-based 2D nanomaterials for efficient visible light-driven ciprofloxacin degradation and overall water splitting, *Energy Convers. Manage.*, 2024, **309**, 118407.
158 N. A. H. Mohammed, *et al.*, Chitosan incorporated nickel ferrite photocatalyst for complete photocatalytic degradation of ciprofloxacin, ampicillin and erythromycin in water, *Results Chem.*, 2024, **7**, 101307.
159 W. Han, *et al.*, Efficient electron transport between NiO/Fe2O3 by loading amorphous carbon improves photocatalytic degradation property, *J. Environ. Chem. Eng.*, 2024, **12**(1), 111667.
160 S. Balu, *et al.*, Advanced photocatalytic materials based degradation of micropollutants and their use in hydrogen production–a review, *RSC Adv.*, 2024, **14**(20), 14392–14424.
161 R. Tsolele, O. Arotiba and S. Malinga, Fabrication of phosphorus-doped graphitic carbonitride towards the photodegradation of ciprofloxacin and sulfamethoxazole, *Int. J. Environ. Sci. Technol.*, 2024, **21**(10), 7009–7023.
162 K. S. A. Sohaimi and J. Jaafar, Influence of calcination temperature on ciprofloxacin photodegradation by vanadium pentoxide/graphitic carbon nitride photocatalyst, *ASEAN Eng. J.*, 2024, **14**(2), 225–230.
163 J. Adorna Jr, *et al.*, Indirect Z-scheme nitrogen-doped carbon dot decorated Bi2MoO6/g-C3N4 photocatalyst for enhanced visible-light-driven degradation of ciprofloxacin, *Chem. Eng. J.*, 2021, **422**, 130103.
164 Y. Wang, *et al.*, Novel carbon quantum dot modified g-C3N4 nanotubes on carbon cloth for efficient degradation of ciprofloxacin, *Appl. Surf. Sci.*, 2021, **559**, 149967.
165 X.-N. Wei, *et al.*, One-pot self-assembly of 3D CdS-graphene aerogels with superior adsorption capacity and photocatalytic activity for water purification, *Powder Technol.*, 2019, **345**, 213–222.
166 D. Yan, *et al.*, Fabrication of carbon nanotube functionalized MIL-101 (Fe) for enhanced visible-light photocatalysis of ciprofloxacin in aqueous solution, *Appl. Surf. Sci.*, 2019, **498**, 143836.
167 J. Yang, *et al.*, Fabrication and tribological properties of self-assembled monolayers of alkanethiols on nickel substrates, *Appl. Surf. Sci.*, 2021, **559**, 149963.
168 J. Luo, *et al.*, Graphitic carbon nitride/ferroferric oxide/reduced graphene oxide nanocomposite as highly active visible light photocatalyst, *Nano Res.*, 2023, **16**(1), 371–376.
169 R. Singh, *et al.*, A critical review on visible light active graphitic carbon nitride (g-CN) based photocatalyst for environment remediation application: A sustainable approach, *J. Clean. Prod.*, 2023, **427**, 138855.
170 S. M. Hossain, *et al.*, Visible light activation of photocatalysts formed from the heterojunction of sludge-generated TiO2 and g-CN towards NO removal, *J. Hazard. Mater.*, 2022, **422**, 126919.
171 S. Danfá, *et al.*, Supported TiO2 in ceramic materials for the photocatalytic degradation of contaminants of emerging concern in liquid effluents: a review, *Molecules*, 2021, **26**(17), 5363.
172 I. Idrees, *et al.*, Silver (Ag) doped graphitic carbon nitride (g-C3N4) photocatalyst for enhanced degradation of Ciprofloxacin (CIP) under visible light irradiation, *Arab. J. Chem.*, 2024, **17**(3), 105615.
173 M. S. Khan, A review of metal–organic framework (MOF) materials as an effective photocatalyst for degradation of organic pollutants, *Nanoscale Adv.*, 2023, **5**(23), 6318–6348.
174 T. Xia, *et al.*, Photocatalytic degradation of organic pollutants by MOFs based materials: A review, *Chin. Chem. Lett.*, 2021, **32**(10), 2975–2984.
175 G. Gunawan, N. B. A. Prasetya and R. A. Wijaya, Degradation of ciprofloxacin (CIP) antibiotic waste using the advanced oxidation process (AOP) method with ferrate (VI) from extreme base electrosynthesis, *Trends Sci.*, 2023, **20**(7), 6639.
176 C. Liu, *et al.*, Recyclable Engineering of Metal–Organic Frameworks toward Sustainable Water Remediation: From Strategies to Applications, *ACS Appl. Mater. Interfaces*, 2025, **17**(35), 49092–49118.
177 T. Irshad, *et al.*, Metal–organic frameworks for energy storage applications: Recent advances, *J. Chin. Chem. Soc.*, 2023, **70**(9), 1692–1714.
178 S. S. A. Shah, *et al.*, Recent trends in wastewater treatment by using metal-organic frameworks (MOFs) and their composites: a critical view-point, *Chemosphere*, 2024, **349**, 140729.

179 H. Ramezanalizadeh and F. Manteghi, Synthesis of a novel MOF/CuWO4 heterostructure for efficient photocatalytic degradation and removal of water pollutants, *J. Clean. Prod.*, 2018, **172**, 2655–2666.
180 C.-K. Tsai, *et al.*, Enhanced Visible-Light-Responsive Photocatalytic Degradation of Ciprofloxacin by the CuxO/Metal-Organic Framework Hybrid Nanocomposite, *Nanomaterials*, 2023, **13**, 282, DOI: 10.3390/nano13020282.
181 S. Thakur and S. Bharti, Recent progress in metal–organic frameworks based nanocomposites for antibiotic removal from water: An in-depth review, *Environ. Sci. Pollut. Res.*, 2025, DOI: 10.1007/s11356-025-36155-3.
182 K. S. Mabape, *et al.*, Sunlight-driven charge separation for a heterojunction of nano-pyramidal CuWO4-MOF modified TiO2 nanoflakes for photocatalytic degradation of ciprofloxacin, *Chem. Pap.*, 2024, **78**(15), 8417–8432.
183 A. Mahmood, *et al.*, Degradation behavior of mixed and isolated aromatic ring containing VOCs: Langmuir-Hinshelwood kinetics, photodegradation, in-situ FTIR and DFT studies, *J. Environ. Chem. Eng.*, 2021, **9**(2), 105069.
184 R. H. A. Murti, *et al.*, High efficiency on resin photocatalysis: Study on application and kinetic mechanism using langmuir Hinshelwood Model, *S. Afr. J. Chem. Eng.*, 2025, **53**, 87–95.
185 E. Siddhardhan, *et al.*, Efficient removal of TC and CIP antibiotics by surface modified g-C3N4/CdS nanocomposite under sunlight irradiation, *Dyes Pigm.*, 2024, **225**, 112052.
186 L. Qirui, *et al.*, Ternary Metal Oxide–Chitosan Hybrids for Efficient Photocatalytic Remediation of Organic Pollutants from Wastewater, *Top. Catal.*, 2025, **68**(9), 984–999.
187 N. Roghani and N. Keramati, Synthesis, photocatalytic activity for tetracycline degradation under visible light, and kinetic study of Ag/AgCl/ZIF-11 nanocomposite, *Environ. Sci. Pollut. Res.*, 2025, **32**(2), 811–832.
188 X. Wu, A Novel High Oxygen Migration Barrier Naw/Nife2o4 Bifunctional Oxygen Carrier for Chemical Looping Oxidative Dehydrogenation Coupled with Co2 Splitting, *J. Environ. Chem. Eng.*, 2025, 119598.
189 N. Azhari, *et al.*, Enhancing the Self-Cleaning Properties of Ball-Milled TiO_2 Nanoparticles: Sustainable Utilization of Natural Rutile and Leucoxene from Thailand, *Case Stud. Constr. Mater.*, 2025, e05247.
190 Y. Dong, *et al.*, Facile fabrication of Zn0. 6Cd0. 4S/ZnO/g-C3N4 dual Z-scheme heterostructures with enhanced performance under visible light: an experimental and theoretical study, *Sci. Rep.*, 2025, **15**(1), 18084.
191 T. Di, *et al.*, Review on metal sulphide-based Z-scheme photocatalysts, *ChemCatChem*, 2019, **11**(5), 1394–1411.
192 D. Zhou, D. Li and Z. Chen, Recent advances in ternary Z-scheme photocatalysis on graphitic carbon nitride based photocatalysts, *Front. Chem.*, 2024, **12**, 1359895.
193 A. Lima, *et al.*, Investigation of ternary catalysts for methanol electrooxidation, *J. Appl. Electrochem.*, 2001, **31**(4), 379–386.
194 M. A. Ahmed and A. A. Mohamed, Recent progress in semiconductor/graphene photocatalysts: synthesis, photocatalytic applications, and challenges, *RSC Adv.*, 2023, **13**(1), 421–439.
195 A. Gnanaprakasam, V. Sivakumar and M. Thirumarimurugan, Influencing parameters in the photocatalytic degradation of organic effluent via nanometal oxide catalyst: a review, *Indian J. Eng. Mater. Sci.*, 2015, **2015**(1), 601827.
196 P. A. K. Reddy, *et al.*, Recent advances in photocatalytic treatment of pollutants in aqueous media, *Environ. Int.*, 2016, **91**, 94–103.
197 H. Zhang, *et al.*, Highly conductive Ti3C2 MXene reinforced g-C3N4 heterojunction photocatalytic for the degradation of ciprofloxacin: Mechanism insight, *Sep. Purif. Technol.*, 2024, **330**, 125520.
198 H. Liu, *et al.*, Pumice-loaded rGO@ MnO2 nanomesh photocatalyst with visible light response for rapid degradation of ciprofloxacin, *Sep. Purif. Technol.*, 2022, **297**, 121502.
199 T. Zhang, *et al.*, Removal of antibiotic-resistant genes during drinking water treatment: A review, *J. Environ. Sci.*, 2021, **104**, 415–429.
200 S. K. Srivastava, Recent advances in removal of pharmaceutical pollutants in wastewater using metal oxides and carbonaceous materials as photocatalysts: a review, *RSC Appl. Interfaces*, 2024, **1**(3), 340–429.
201 S. P. Gupta and S. K. Samanta, Thermal activation of persulfate for degradation of ciprofloxacin in water: Mechanism, influencing factors and toxicity assessment, *J. Water Proc. Eng.*, 2025, **72**, 107646.
202 Y. Chen, *et al.*, Toward a fundamental understanding of factors affecting the function of cocatalysts in photocatalytic water splitting, *Curr. Opin. Green Sustainable Chem.*, 2019, **17**, 21–28.
203 N. A. A. Aziz, *et al.*, Review of the mechanism and operational factors influencing the degradation process of contaminants in heterogenous photocatalysis, *J. Chem. Res.*, 2016, **40**(11), 704–712.
204 M. A. Hassaan, *et al.*, Central composite design and mechanism of antibiotic ciprofloxacin photodegradation under visible light by green hydrothermal synthesized cobalt-doped zinc oxide nanoparticles, *Sci. Rep.*, 2024, **14**(1), 9144.
205 R. Gusain, N. Kumar and S. S. Ray, Factors influencing the photocatalytic activity of photocatalysts in wastewater treatment, *Photocatalysts in Advanced Oxidation Processes for Wastewater Treatment*, 2020, pp. 229–270.
206 T. Hayri-Senel, *et al.*, Photocatalytic degradation of ciprofloxacin from water with waste polystyrene and TiO2 composites, *Heliyon*, 2024, **10**(3), e25433.
207 H. Taha, A. Zaher and N. Shehata, Optimization and kinetic modeling of ciprofloxacin adsorption and photocatalytic degradation in water, *Sci. Rep.*, 2025, **15**(1), 43370.
208 W. S. Koe, *et al.*, An overview of photocatalytic degradation: photocatalysts, mechanisms, and development of

photocatalytic membrane, *Environ. Sci. Pollut. Res.*, 2020, **27**(3), 2522–2565.

209 C. Zhou, *et al.*, Strategies for enhancing the perylene diimide photocatalytic degradation activity: method, effect factor, and mechanism, *Environ. Sci.: Nano*, 2021, **8**(3), 602–618.

210 S. Aghdasi and M. Shokri, Photocatalytic degradation of ciprofloxacin in the presence of synthesized ZnO nanocatalyst: The effect of operational parameters, *Iran. J. Catal.*, 2016, **6**(5), 481–487.

211 S. John, *et al.*, Solar-driven hybrid photo-Fenton degradation of persistent antibiotic ciprofloxacin by zinc ferrite-titania heterostructures: degradation pathway, intermediates, and toxicity analysis, *Environ. Sci. Pollut. Res.*, 2023, **30**(14), 39605–39617.

212 F. Tamaddon, A. Nasiri and G. Yazdanpanah, Photocatalytic degradation of ciprofloxacin using CuFe2O4@ methyl cellulose based magnetic nanobiocomposite, *MethodsX*, 2020, **7**, 100764.

213 A. K. Al-Buriahi, *et al.*, Ciprofloxacin removal from non-clinical environment: A critical review of current methods and future trend prospects, *J. Water Proc. Eng.*, 2022, **47**, 102725.

214 S. Manna, N. Remya and N. Singhal, Advancements in S-scheme photocatalytic material for wastewater treatment, *J. Environ. Chem. Eng.*, 2023, **11**(3), 109838.

215 S. Pourali, *et al.*, In situ synthesis of ZnO/g-C3N4 based composites for photodegradation of methylene blue under visible light, *Sci. Rep.*, 2025, **15**(1), 462.

216 X. Bai, *et al.*, Photocatalytic degradation of some typical antibiotics: Recent advances and future outlooks, *Int. J. Mol. Sci.*, 2022, **23**(15), 8130.

217 P. N. Thanh, V.-D. Phung and T. B. Nguyen, Recent advances and future trends in metal oxide photocatalysts for removal of pharmaceutical pollutants from wastewater: a comprehensive review, *Environ. Geochem. Health*, 2024, **46**(9), 364.

218 N. Syed, J. Huang and Y. Feng, CQDs as emerging trends for future prospect in enhancement of photocatalytic activity, *Carbon Lett.*, 2022, **32**(1), 81–97.

219 J. Ma, *et al.*, Recent advances in photocatalytic degradation of tetracycline antibiotics, *Catalysts*, 2024, **14**(11), 762.

220 A. Majeed, M. A. Iqbal and T.-O. Do, Advances in Composite Photocatalysts for Efficient Degradation of Organic Pollutants: Strategies, Challenges, and Future Perspectives, *Catalysts*, 2025, **15**(9), 893.

221 R. Arya, A. Garg and S. Majumder, Removal of ciprofloxacin and amoxicillin from wastewater using photocatalysis and biological treatment methods: a mini review, *Int. J. Chem. React. Eng.*, 2025, **23**(7), 755–776.

222 H. H. Shanaah, *et al.*, Photocatalytic degradation and adsorptive removal of emerging organic pesticides using metal oxide and their composites: Recent trends and future perspectives, *Sustainability*, 2023, **15**(9), 7336.

223 A. H. da Silva Júnior, *et al.*, Reviewing perovskite oxide-based materials for the effective treatment of antibiotic-polluted environments: challenges, trends, and new insights, *Surfaces*, 2024, **7**(1), 54–78.